

# Corneal Imaging Revisited: An Overview of Corneal Reflection Analysis and Applications

CHRISTIAN NITSCHKE<sup>1,a)</sup> ATSUSHI NAKAZAWA<sup>1,2</sup> HARUO TAKEMURA<sup>1</sup>

Received: September 27, 2011, Accepted: October 25, 2012

**Abstract:** The cornea of the human eye acts as a mirror that reflects light from a person's environment. These corneal reflections can be extracted from an image of the eye by modeling the eye-camera geometry as a catadioptric imaging system. As a result, one obtains the visual information of the environment and the relation to the observer (view, gaze), which allows for application in a number of fields. The recovered illumination map can be further applied to various computational tasks. This paper provides a comprehensive introduction on corneal imaging, and aims to show the potential of the topic and encourage advancement. It makes a number of contributions, including (1) a combined view on previously unrelated fields, (2) an overview of recent developments, (3) a detailed explanation on anatomic structures, geometric eye and corneal reflection modeling including multiple eye images, (4) a summary of our work and contributions to the field, and (5) a discussion of implications and promising future directions. The idea behind this paper is a geometric framework to solve persisting technical problems and enable non-intrusive interfaces and smart sensors for traditional, ubiquitous and ambient environments.

**Keywords:** catadioptric imaging, corneal imaging, geometric eye model, eye gaze tracking (EGT), human-computer interaction (HCI)

## 1. Introduction

Our eyes are one of the most important sense organs, allowing the exploration, analysis, perception of, and interaction with the visual information content of the physical world. Therefore, the eye and its movements provide a key contribution to interpreting and understanding a person's wishes, needs, tasks, cognitive processes, affective states and interpersonal relations. The unique geometric and photometric properties of the eyes provide important visual cues for obtaining face-related information; their unique appearance is exploited in biometrics and computer graphics. Image-based eye analysis allows for non-intrusive measurement of eye structures and visual acuity in optometry, and diagnosis of diseases and disorders of the visual system in ophthalmology.

**Corneal reflections and applications.** The cornea is the transparent protective and optical outer layer of the eye that covers the iris and accounts for the majority of the eye's optical power. While light arriving at its surface mainly refracts and enters the eye, a small part reflects back into the environment and can be noticed when looking at a person's eye (**Fig. 1**). Analyzing and exploiting such corneal reflections from eye images can be beneficial to accomplish a wide range of tasks that involve information about the environment (scene panorama/model) and the relationship with the observer (eye pose). For example, this al-

lows us to determine the situation under which a person is photographed (forensics, surveillance), to calculate a person's field of view and point of gaze (PoG) (sensing, human-computer interaction (HCI)), and to perform higher-level analysis of stimulus and response that may enable novel insights and interface concepts. The recovered illumination map can be further applied to various computational tasks in vision and graphics (face modeling/relighting, biometrics, image forensics).

**Issues and potential.** While corneal imaging enables catadioptric vision [137], the cornea is not a perfect mirror and suffers from several issues including (1) a low resolution from the small size and large field of view of the corneal mirror, (2) a low contrast as the reflectivity of the cornea is less than 1% [82], (3) a contamination with iris texture reflections [130] as the cornea is transparent, and (4) distortions from an unknown individual shape that is not handled by simple eye models. The low reflectivity further makes image acquisition challenging, as it requires a long exposure and opened aperture, which causes motion and defocus blur. Regarding these issues, corneal imaging will not replace high-quality catadioptric systems, but enable gathering information when only face/eye images are available or when the relationship between a person and the environment is concerned. An advantage is the minimum requirement of only a single face image that provides a distinct view of the scene from each eye, which allows for dynamic and real-time scenarios.

**Corneal reflection analysis** benefits from theories and techniques in catadioptric imaging [115], but at the same time demands for specialized algorithms that handle and exploit the unique properties of the eye. Regarding the complexity of the problem, the majority of algorithms either completely refrains

<sup>1</sup> Cybermedia Center, Osaka University, Toyonaka, Osaka 560-0043, Japan

<sup>2</sup> PRESTO, Japan Science and Technology Agency (JST), Kawaguchi, Saitama 332-0012, Japan

<sup>a)</sup> christian.nitschke@cmc.osaka-u.ac.jp



**Fig. 1** Corneal reflections. (a) View from the side onto the transparent reflective cornea. (b) A close view reveals the corneal limbus as the surface shape discontinuity, where the cornea dissolves into the white sclera. (c) The reflected office environment is clearly visible in the eye image. Diffuse iris reflections are superimposed with specular corneal reflections. (d) Focus on iris texture instead of corneal reflections. (e), (f) Examples of corneal images and corresponding (fisheye) images for different scenes.

from geometric modeling or applies a substantial simplification, which sacrifices quality, usability and applicability. Nevertheless, geometric techniques become increasingly popular. Nishino and Nayar [83] establish the fundamentals of corneal imaging with a comprehensive analysis of the visual information about the environment that is embedded within a single image of an eye. While corneal reflection analysis has a great potential, present advancement is limited by several factors that need to be handled. These include (1) the low quality of corneal images (resolution, reflectivity, iris texture), (2) the unknown characteristics of the individual eye (shape, appearance), (3) the establishment of reliable automatic modeling techniques, and (4) the integration of multiple eye and scene images (correspondence matching) with available domain knowledge.

**Scope and contribution.** With the aim to raise awareness for the problem and encourage novel development, this paper provides a comprehensive introduction on corneal imaging, covering three major parts: (1) A review of existing applications in various fields showcases the wide range of the topic and summarizes the state-of-the-art (Section 2). (2) An introduction to the anatomic background, followed by a detailed description of geometric eye modeling (Section 3), eye pose estimation (Section 4) and catadioptric modeling (Section 5), provides engineers with tools for algorithm design and implementation. (3) Finally, a broad discussion of our work and contributions to the field (Section 6), implications (Section 7) and promising future directions (Section 8), highlights strategies for novel techniques and applications. The key idea is a geometric framework that integrates the modeling of cameras, eyes, illumination and scene structure, using multiple images and domain knowledge, and allows a flexible combination of constraints and unknowns to solve various tasks.

## 2. Applications

It follows an overview on particular applications and problems involving corneal reflection analysis.

### 2.1 Information about the eye

**Eye gaze tracking (EGT)** is the problem of measuring and tracking the pose of the eye or the PoG in the scene. Tech-

niques commonly exploit eye features and specular highlights. Early approaches do not model the eye geometry, and perform a calibration to map the distance between the pupil center and a single highlight to the PoG on a planar surface [73], [112]. The strategy does not support head movement and, thus, requires rigid body attachments or head motion compensation. Recent remote approaches apply a 3D geometric eye model and estimate its pose using imaged eye features and highlights from multiple light sources at known positions. Passive methods track anatomic eye features and estimate the gaze direction, either directly [83], [101], [131], [134] or in conjunction with the head pose [95], [138]. However, for increased accuracy and robustness the majority of methods applies active illumination using IR LEDs [37], [106], [127], [129]. The PoG is commonly recovered as the intersection of the gaze ray with a scene model. If unknown, scene information may be directly obtained from corneal reflections, e.g., for a planar display from attached LEDs [43], [53] or screen content [43], [87], [101], and for arbitrary scenes using catadioptric back-projection [83] or forward-projection [78], [84]. Geometric methods often require high-resolution eye images that are obtained using stationary high-resolution cameras, dynamic pan-tilt-zoom (PTZ) cameras [95], [139] or mirrors [56].

**Corneal shape measurement.** Corneal reflection analysis requires a known pose and shape for the cornea. Commonly applied are spherical models with fixed size or personal parameters recovered using multiple cameras. Only a few approaches support spheroid, ellipsoid or general rotational symmetric models that better describe the corneal periphery [10], [77], [83]. There exist several non-intrusive optical techniques to measure corneal shape and geometry in the context of ophthalmology and optometry: Keratometry (ophthalmometry) considers the cornea to be a spherical reflective surface and measures its radius of curvature. The calculation is based on geometric optics, applied to only four sampling points in a small portion of the central cornea. More accurate shape models may be reconstructed through reflections from controlled illumination using the principle of shape from specular reflection [8], [48]. Photokeratometry, or videokeratography, [42], [70], [118] is a diagnostic technique that applies

this principle to reconstruct accurate models of corneal topography [11], [32] for various medical applications, such as refractive surgery, change monitoring, disease diagnosis and contact lens development. The technique works as follows: A patient is seated in front of a keratographer, a concave device that displays an illuminated pattern (commonly a series of concentric rings or a moving slit light). The pattern is focused on the anterior surface of the patient’s cornea and reflected back to a digital camera at the center of the pattern. This allows to reconstruct the shape of the whole cornea from the distortion of the reflected pattern at several thousand sampling points. The result can be represented in a number of formats, such as an axial, tangential, elevation or refractive map, to visualize different characteristics of corneal topography.

**Separation of corneal reflections and iris texture.** A large part of the light entering the eye diffusely reflects off the iris, especially in blue or green eyes. When taking an image of an eye, such iris texture reflections superimpose on corneal reflections, which causes noise in the extraction of both types. Therefore, Wang et al. [130] introduce a separation method that exploits the physical characteristics of a pair of irises. The recovered iris texture is important, e.g., for iris recognition in biometrics [22], [133] and iris synthesis in computer graphics [59], [64]. While the aim of this research is to remove corneal reflections from iris images, it may also be used to remove iris texture from corneal images.

**2.2 Information about the environment**

A known pose and shape for the cornea enables modeling the cornea-camera geometry as a catadioptric imaging system to recover the environmental illumination and apply it to various tasks in vision and graphics. This is commonly referred to as *corneal imaging*.

**Environmental light map.** Tsumura et al. [123] are the first to recover the direction of environmental illumination from specular highlights in the eye and apply it to face reconstruction and relighting. Johnson and Farid [51] describe a method to reveal digital forgeries, where images are composed from persons photographed under different illumination. The method can be applied with any arbitrary photo as it automatically estimates the internal camera parameters from the perspective distortion of the iris contour. Backes et al. [5] describe an image-based eavesdropping technique for recovering reflected content from computer displays at faraway locations. For this purpose, they analyze the point spread function of the corneal reflection system and intro-

duce a non-blind deconvolution method. Nishino and Nayar [83] provide the first comprehensive analysis of the visual information about the environment that is embedded within an image of the human eye. Their seminal study formalizes the combination of camera and corneal reflector as a catadioptric imaging system, derives its imaging characteristics and describes its calibration. The recovered environment map allows for a number of interesting applications, such as the computation of a scene panorama and a subject’s view, as well as face reconstruction, relighting [82] and recognition [81]. Recent science fiction works showcase several exciting applications [91], [94]. For example, by applying corneal imaging to a surveillance video footage that shows a persons’s facial region, they obtain detailed information about the surrounding scene, revealing a criminal’s face or printed fabric patterns the person looks at.

**Scene structure.** The two eyes, captured in a single face image, form a catadioptric stereo system that enables reconstruction of simple 3D structure [83]. Recently, it has been shown that the pose of a planar computer screen can be estimated from reflected point [87] or line features [101] using multiple eye poses. The combination of display, eyes and camera allows for applications in different fields, including HCI [44], [60], surveillance and forensics [5], graphics and vision [82], [83], [123], and medicine [92], [93].

**3. Eye anatomy and model**

The following section reviews important anatomic structures and introduces a geometric eye model for pose estimation and reflection modeling.

**3.1 The human eye**

The human eye is the organ that provides the optics and photo-reception for the visual system—and the anatomy follows its function in this physiological process. An outer view of the eye in Fig. 2 (a) shows the color-textured iris and the pupil in its center as the most distinctive components. The iris is surrounded by the white sclera, a dense and opaque fibrous tissue that mainly has a protective function.

**3.1.1 Eyeball**

A cross section of the eyeball in Fig. 2 (b) reveals that its main part is located behind the skin and components visible from the outside. Geometrically, the eyeball is not a plain sphere; its outer layer can be subdivided into two approximately spherical segments with different radii and separated centers of curvature: the

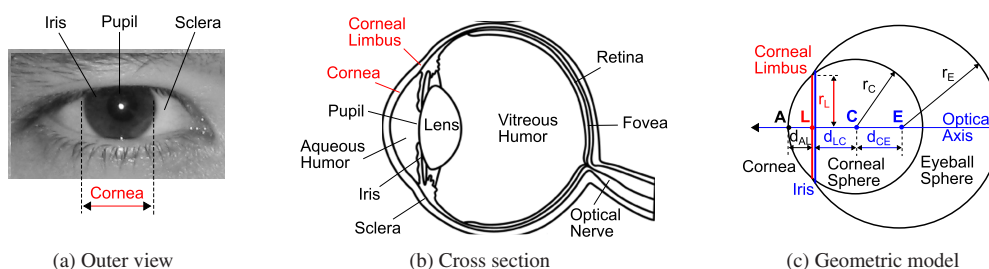


**Fig. 2** Eye model. (a) Outer view and (b) cross section of the human eye with important components marked red. (c) Approximation by a spherical eye model with static parameter values, highlighting components involved in eye pose estimation.

**Table 1** Eye parameter variation [mm].

	Eyeball			Posterior	Anterior			
	$d_{AL}$	$d_{LC}$	$d_{CE}$	$r_E$	$r_C$	$r_L$	$r_{LH}$	$r_{LV}$
(a) Books on eye anatomy								
Snell & Lemp [109]	—	—	—	12.00	7.70	5.575*	5.85	5.30
Crick & Khaw [21]	—	—	—	—	—	5.75*	6.00	5.50
Kaufman & Alm [54]	—	—	—	—	7.80	6.075*	6.30	5.85
Remington [96]	—	—	5.70	12.00	7.80	5.75*	6.00	5.50
Khurana [55]	—	—	—	12.00	7.80	5.675*	5.85	5.50
(b) Schematic eye models								
Gullstrand [39] No. 1	3.60	—	—	—	7.80	—	—	—
Gullstrand [39] No. 2	3.70	—	—	—	7.70	—	—	—
Le Grand & El Hage [63] 1945	3.60	—	—	12.30	7.80	—	—	—
Lotmar [69]	3.60	—	—	12.30	7.80	—	—	—
Kooijman [58]	3.55	—	—	—	7.80	—	—	—
Liou & Brennan [68]	3.66	—	—	—	7.77	—	—	—
Escudero-Sanz & Navarro [26]	3.60	—	—	12.00	7.72	—	—	—
(c) Work on eye modeling and applications								
Lefohn et al. [64]	2.50	5.25	4.70	11.50	7.80	5.80	—	—
Johnson & Farid [51]	—	—	—	—	—	—	—	—
Morimoto & Mimica [75]	3.53*	4.17	—	—	7.70	6.47*	—	—
Hua et al. [47]	—	—	—	12.50	7.80	5.50	—	—
Nishino & Nayar [82], [83]	2.18	—	—	—	7.80	5.50	—	—
Li et al. [67]	3.05	4.75*	5.70*	12.50*	7.80	6.19*	—	—
This study	2.27*	5.53*	5.70	—	7.80	5.50	—	—

\*Calculated from given values.

**Table 2** Anatomic zones of the cornea (adapted from Ref. [109]).

Corneal zone	Approximate diameter [mm]	Characteristics
Central optical	0-4	most spherical, symmetric; overlies pupil
Paracentral (mid)	4-7	generally spherical, but progressive flattening
Peripheral	7-11	greatest flattening and asphericity
Limbal	11-12	cornea steepens before joining the sclera

anterior corneal and the posterior scleral segment (Fig. 2 (c)). The smaller anterior segment covers about one-sixth of the eye, and contains the components in front of the vitreous humor, including the cornea, aqueous humor, iris, pupil and lens. It has a radius of curvature  $r_C$  of  $\sim 8$  mm. The posterior segment covers the remaining five-sixths with a radius of curvature  $r_E$  of  $\sim 12$  mm. Both centers of curvature are separated by a distance  $d_{CE}$  of  $\sim 5$  mm. The eyeball is not symmetric; its diameters are approximately 23.5 mm horizontal ( $d_H$ ), 23 mm vertical ( $d_V$ ), and 24 mm antero-posterior ( $d_{AP}$ ) (distance between anterior pole at the apex of the cornea and posterior pole at the retina) [96]. See **Table 1** for an overview of parameter values from different sources.

The eye has several axes, where the optical and visual axes are the two major ones. The optical axis is usually defined as the line joining the centers of curvature of the refractive surfaces, connecting the corneal apex **A**, limbus center **L**, corneal center **C** and eyeball center **E**. The visual axis describes the gaze direction of the eye. It is defined as the line joining the fovea and the object being viewed, which slightly differs from the optical axis. Both axes intersect at the nodal point of the eye, where the image of the gazed object becomes reversed and inverted. For a typical adult, the deviation of the visual axis is  $4^\circ$ – $5^\circ$  nasal and  $1.5^\circ$  superior to the optical axis with a standard deviation of  $3^\circ$  [44].

**3.1.2 Cornea**

The transparent cornea is the outer layer of the eye that covers the iris and dissolves into the sclera at the corneal limbus. Beside having a protective function the cornea plays the main role

for the eye as an optical system to focus images on the retina. Its transparency and optical clarity stem from three factors [21], [54]: (1) the uniform size and arrangement of submicroscopic collagen fibrils, (2) the absence of blood vessels (avascularity), and (3) the relative state of dehydration. The internal pressure of the eye is higher than that of the atmosphere, which maintains the corneal shape and produces a smooth external surface. In addition, the surface is coated with a thin film of tear fluid that ensures its smoothness and helps to nourish the cornea. As a result, the surface shows mirror-like reflection characteristics.

Although the corneal surface is approximately a sphere, it has only spherical curvature near the apex and generally flattens towards the periphery. The cornea is subdivided into four anatomic zones with an increasing radius from the optical axis (**Table 2**). The eyeball is usually not rotationally symmetric around the optical axis but slightly flat in the vertical direction. This leads to a toricity in the corneal surface with a higher vertical curvature. There occurs a considerable individual variation in eye surface curvature, component separation and axial length. The typical cornea approximates to an ellipsoid, with an apex radius of curvature  $r_C$  of about 7.8 mm. Asphericity values for individual eyes are widely distributed and can include some cases where the cornea steepens rather than flattens towards the periphery.

**3.1.3 Corneal limbus**

The area where the transparent cornea dissolves into the opaque sclera is called the corneal or corneoscleral limbus. It is a band, approximately 1.5–2.0 mm wide, that surrounds the pe-

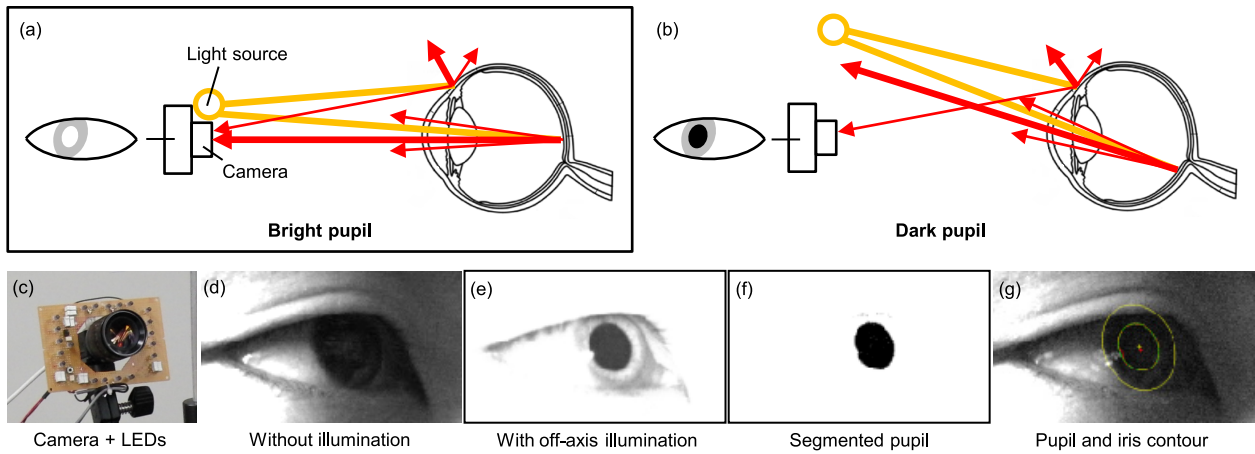


**Fig. 3** Pupil segmentation and iris contour fitting. (a) Bright-pupil effect from on-axis illumination, also known as red-eye effect in flash photography. (b) Dark-pupil effect from off-axis illumination. (c) Camera with off-axis IR LEDs. (d) Eye image without LED illumination. (e) Off-axis illumination creates a dark pupil. (f) Segmented pupil from difference image. (g) Segmented pupil contour (red), and fitted ellipses to pupil (green) and iris contours (yellow).

riphery of the cornea [96], [109]. The radius of curvature immediately changes at this intersection, creating a shallow groove with a shape discontinuity on the outer surface of the eye. Refer to Table 1 for an overview of common values for the horizontal radius  $r_{LH}$ , vertical radius  $r_{LV}$ , and mean radius  $r_L$  of the limbus.

Histologically, the limbus contains the transition from the regular lamellar structure of collagen fibrils of the cornea to the irregular and random organization of collagen bundles in the sclera. The layers of corneal tissue either merge into scleral tissue or terminate at different landmarks. The limbal area further contains blood vessels and lymphatic channels. This leads to a smooth and non-uniform transition.

### 3.1.4 Iris

The iris is a thin, pigmented, circular structure located directly in front of the lens. Its mean radius  $r_I$  is 6 mm. The outer structures of the iris extend behind the limbus and the beginnings of the sclera. The area visible on the outside is delimited by the transparent corneal tissue that inhomogeneously dissolves at the limbus.

Iris colors for normal eyes range from light blue to dark brown, depending on the arrangement and density of the connective tissue and pigment. The color may vary between both eyes of the same person and different parts of the same iris [109]. The surface of a heavily pigmented brown iris appears smooth and velvety, whereas the surface of a lightly colored gray, blue, or green iris appears rough and uneven.

### 3.1.5 Pupil

The iris forms the diaphragm of the optical system with a central circular aperture, the pupil. The size of the pupil controls retinal illumination with a diameter varying between 1 and 8 mm. In about 25% of individuals it slightly differs in size [109]. The image of the pupil seen on the outside is a virtual image corresponding to the entrance pupil that is forward to and slightly larger than the real pupil [4]. Compared to the smooth appearance of the iris boundary, the circular pupillary margin is a rather sharp edge. The pupil appears black, because most of the entering light is absorbed by the tissues of the inner eye. The pupil can appear red

in an image when the eye is photographed in low-intensity ambient light under a bright flash illumination. This so-called *red-eye effect* is caused by the large amount of light, reflected from the back of the eyeball in the direction of the camera, when the flash is located near the lens (Fig. 3 (a)).

## 3.2 Geometric eye model

Knowledge of the shape and parameter distribution of the human eye allows for the construction of eye models. Several so-called schematic eye models with different levels of sophistication have been developed over the last 150 years; motivated by the aim to describe the imaging characteristics and performance of the eye as an optical system [39], [58], [63], [68], [69].

For applications related to corneal imaging, it is sufficient to model the outer (visible) surface of the eye, which does not require dealing with refractive surfaces of the inner eye. The most common approach in eye modeling is to represent the eyeball as two overlapping spheres with different radii and separated centers of curvature, **C** and **E** (Fig. 2 (c)) [32]. For reference, the applied parameter values are listed in Table 1. The cornea is modeled as a spherical cap, with a radius of curvature  $r_C$  of 7.8 mm [54], that is cut off from the corneal sphere by the limbus plane<sup>\*1</sup>. The visible part of the iris is assumed to be equal to the circular limbus, with a mean radius  $r_L$  of 5.5 mm [83]. The displacement  $d_{LC}$  between the centers of the limbal circle and the corneal sphere are obtained from the given parameters as in

$$d_{LC} = \sqrt{r_C^2 - r_L^2} \approx 5.53 \text{ mm.} \quad (1)$$

The height of the cornea, defined as the distance  $d_{AL}$  between the corneal apex **A** and the center of the circular limbus **L**, is obtained as in

$$d_{AL} = r_C - d_{LC} \approx 2.27 \text{ mm.} \quad (2)$$

<sup>\*1</sup> For more complex aspherical representations of corneal curvature refer to Refs. [4], [7], [10], [77], [83].

**Table 3** Comparison of eye pose/gaze estimation methods. The column “Cameras” indicates the number of cameras per eye, where “+” refers to additional wide field-of-view cameras and “\*” to the use of continuous video frames. The column “Lights” indicates the number of IR LED light sources, where “+” refers to additional sources for redundancy. The column “Personal calibration [pts]” indicates the number of points required for calibrating personal parameters such as the visual axis offset, eye size and cornea–pupil distance. There exist automatic approaches that minimize either §(1) the re-projection error from a 3D face/eye model or §(2) the error from geometric scene constraints. The columns “Gaze information” and “Gaze error [deg]” indicate the obtained axis of the eye and the corresponding error (mean, standard deviation, range). Iris-contour based eye pose estimation commonly results in a two-way ambiguity that is resolved using either †(1) parallel gaze directions in two irises, †(2) equal distance between eyeball center and eye corners, †(3) manual resolution, or †(4) distance between gaze ray–display intersections. Additional information: ‡(1) Head-mounted. ‡(2) Stereo head camera + pan-tilt stereo gaze camera. ‡(3) Head camera + pan-tilt gaze camera. ‡(4) Head camera + pan-tilt-zoom gaze camera. ‡(5) In conjunction with a pan-tilt camera system. ‡(6) Low-resolution images, no intrinsic calibration required. Empty cells indicate that no information is available.

Ref.	Cameras	Lights	Personal calibration [pts]	Gaze information	Gaze error [deg]	Eye pose estimation method		Note
						Eye position	Gaze direction	
(a) Passive, academic								
[131]	1+1	—	—	Optical	0.86±0.16	Eye model	Iris contour <sup>†(1)</sup>	‡(3)
[132]	1+1	—	—	Optical	0.48±0.09	Eye model	Iris contour <sup>†(2)</sup>	‡(4)
[134]	1	—	—	Optical	7.12±4.65	—	Iris contour <sup>†(1)</sup>	‡(5)
[83]	1	—	—	Optical	5.95	Eye model	Iris contour <sup>†(3)</sup>	
[138]	1*	—	§(1)	Optical	9.19±1.48	Image re-projection error from 3D face/eye model		‡(6)
[17]	1*	—	9	Visual	3.34	Eye corners	Pupil center	
[101]	1	—	§(2)	Optical	2.28±0.40	Eye model	Iris contour, scene constraints <sup>†(4)</sup>	
[95]	1	—	4	Visual	1.09±0.67	Calibration + 3D face pose	Iris back-projection error to 3D eye model	‡(3)
(b) Active-light, academic								
[90]	1	1	4	Visual	0.70±0.13	Single CR, depth from focus	Pupil contour	
[10]	2+2	2	≥2	Visual	0.60	Model fitting using multiple CRs + pupil contour		‡(2)
[46]	1	2	4	Optical	0.73±0.13	Multiple CRs	Pupil contour	
[37]	1	2	9	Visual	0.63±0.10	Multiple CRs	Pupil center	
[127]	1	2	1	Visual	1.08±0.23	Multiple CRs	Pupil contour	
[129]	1	2	5	Visual	1.57±0.51	Multiple CRs	Pupil center	
[38]	2	2+2	1	Visual	0.50±0.07	Multiple CRs	Pupil center	
(c) Active-light, commercial								
[107]	1		any	Visual	0.50	Multiple CRs	Head-model + iris/pupil contour	
[105]	1		2/5/9	Visual	0.40	Multiple CRs	Pupil	
[104]	1		5	Visual	<0.50-1.00	Multiple CRs	Pupil	‡(1)
[110]	1			Visual	0.50	Multiple CRs	Pupil	
[111]	1			Visual	<0.50	Multiple CRs	Pupil center	‡(1)
[121]	1		≥2	Visual	0.50	Multiple CRs	Pupil	
[120]	1		9	Visual		Multiple CRs	Pupil center	‡(1)

All eye movements are described as rotations around the geometric center of the eye **E**, located at a distance  $d_{CE}$  of approximately 5.70 mm posterior to the center of the corneal sphere [96], where the limited set of anatomically possible eye poses is described by Donder’s and Listing’s laws [124]. Corneal reflection analysis, however, does not require modeling the surface of the eyeball and eye movements.

#### 4. Eye pose estimation

The following section covers the position and orientation estimation of the eye model relative to the camera, which is equivalent to calibrating the cornea-camera catadioptric imaging system. Eye pose estimation recovers the gaze direction up to the optical axis. An additional one-time individual calibration with at least a single calibration point is necessary to recover the offset to the true gaze direction or visual axis [38], [128]. **Table 3** shows an overview of different methods, mostly related to EGT. Accuracy is indicated as the error in gaze direction, a common measure that relates to the pose of the eye and, thus, to the position of the cornea.

Eye pose estimation requires two tasks: *image processing* and *geometric modeling*. Image processing determines if and where an eye occurs in the image, and tracks the detailed location of particular features that can be real anatomic structures or corneal

reflections (glints). Image-based eye detection and tracking is a large topic with a broad range of approaches. Refer to Ref. [44] for a recent survey. Geometric modeling comprises algorithms that estimate the 3D pose of a geometric eye model from the image information. In the following, we distinguish between *passive methods* that work on any eye image and *active-light methods* that require additional controlled illumination.

##### 4.1 Active-light methods

Active-light methods are developed for accurate automatic eye gaze tracking and require a complex hardware system with calibrated light sources and eye parameters<sup>\*2</sup>. The pupil-center–corneal-reflections (PCCR) technique is largely covered in research [37], [90], [106], [127], [129] and the method of choice in commercial systems [104], [105], [107], [110], [111], [120], [121]. The technique involves a two-step approach, first estimating the position of the cornea from light reflections of multiple light sources at known locations, commonly in the form of IR LEDs [37], [127]<sup>\*3</sup>. Additionally using multiple cameras enables

<sup>\*2</sup> Another advantage of using corneal reflections is the possibility to recover an individual aspheric model of the cornea to further increase the accuracy [77].

<sup>\*3</sup> While current methods apply artificial light sources, future methods may directly exploit scene illumination and structure.



Fig. 4 Limbus-based eye pose estimation, with iris contour (red ellipse), iris center (red mark), corneal center (green mark) and gaze direction (green line).

recovering individual anatomic parameters. In a next step, the orientation of the eye model is obtained by detecting a second point on the optical axis, commonly using the center or contour of the pupil. Pupil segmentation is often realized using active IR illumination to exploit the bright (red-eye) and dark pupil effects [2], [25], [74] (Fig. 3). The strength of either effect depends on different factors, such as the opening of the iris, and the age and ethnicity of the subject. Only a few methods exist that operate under visible light [126], [138], because of the reduced contrast of the pupil contour [36]. Instead of using segmentation, the pupil contour can be obtained through a radial search from a starting point within the pupil. A popular iterative algorithm for this purpose is the *Starburst* algorithm [66].

#### 4.2 Passive methods

Due to their reduced hardware and calibration requirements, passive methods are often applied in low-cost non-professional solutions for EGT and other applications. They work on natural eye images, but suffer from noisy eye detection and unknown parameters. Using multiple cameras enables to recover individual anatomic parameters and further constrains the gaze direction [10], [57], [127]. Passive methods commonly estimate the pose of the eye from the contour of the iris [83], [87], [101], [131], [134], possibly in conjunction with other features, such as eye corners [132], [135] and lids [135].

**Iris tracking.** Although there exists individual variation, the iris is approximately circular. Under perspective projection, a circle with an arbitrary 3D pose maps to a general ellipse in an image [45], [103]. Methods for iris segmentation are proposed in the context of eye tracking [44], iris recognition [13], [71] and medical imaging [9], [49], [50]. The methods either directly fit a shape model to continuous image features, such as intensity gradients and edge distances [3], [83], or first segment a particular feature and subsequently fit a shape model using least squares [27], [41]. Regarding the latter, common strategies apply a vertical edge operator to an upright face image [20], [132] or perform contour detection along radial directions starting at the approximate center [9], [49], [50]. There also exist variations of the *Starburst* algorithm in pupil contour detection that do not require the starting point to be the approximate center [95], [97].

**Limbus pose estimation.** The pose of the eye model is defined by the pose of the circular limbus, that is described by the cen-

ter point  $\mathbf{L} = (L_x, L_y, L_z)^T$  and the normal vector  $\mathbf{g} = (g_x, g_y, g_z)^T$ . Eye pose estimation aims in recovering these values. As the corneal limbus coincides with the contour of the visible iris, its pose is obtained from the elliptical contour of the imaged iris. There exists a large body of works on closed-form solutions to the monocular reconstruction of circles with application to camera and object pose estimation [52], [98], [142]. Multiple parallel or coplanar circles additionally allow for increased stability [40] and estimating camera parameters [18]. These works are the basis for several limbus pose estimation algorithms [84], [101], [131], [134]. A simpler method assuming weak perspective projection may be applied when the distance between the eye and the camera is much larger than the scale of the eye, such as in common people or face photography [83], [87]. Using a single camera, the 3D pose of a circle is estimated up to a two-way ambiguity that is resolved through further knowledge. In the context of eye pose estimation, such constraints are obtained (1) for a single eye image from anthropometric properties [132] or by assuming a gaze direction towards the camera [51], (2) for a single face image by assuming parallel irises when focusing far-away objects [131], [134] or an intersection of the gaze rays at a known display plane [101], (3) and for multiple face images using geometric scene constraints [87]. **Figure 4** shows results of limbus-based eye pose estimation for different subjects and reflected scenes.

**Cornea position.** The cornea is modeled as a spherical surface, described by the radius  $r_C$  and center  $\mathbf{C}$ , located at a distance  $d_{LC}$  from the limbus center  $\mathbf{L}$ , and obtained as in

$$\mathbf{C} = \mathbf{L} - d_{LC} \mathbf{g}. \quad (3)$$

## 5. Corneal reflection modeling

This section builds on eye modeling and pose estimation to describe the back-projection for the cornea-camera catadioptric imaging system. This includes a reflection model to determine the direction towards a light source and the triangulation of rays under multiple eye poses to recover the corresponding light source position. After that, we give an overview of the forward-projection problem.

### 5.1 Cornea-camera catadioptric imaging system

A camera capturing an image of the eye that exhibits corneal reflections of the environment can be modeled as a catadioptric

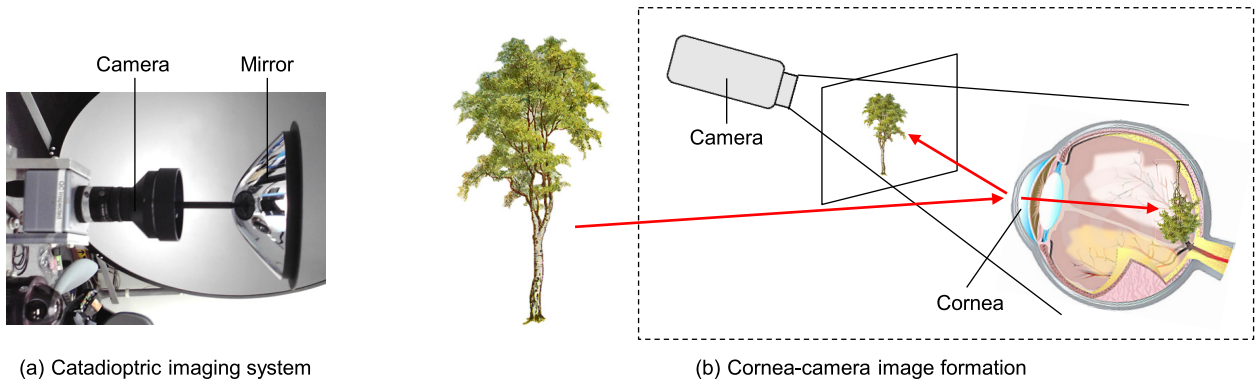


**Fig. 5** Catadioptric imaging. (a) Catadioptric imaging system, where light from the scene reflects at the mirror into the camera. (b) The largest part of light arriving at the cornea refracts and enters the eye. The remaining part reflects back into the environment. When captured by a camera, the compound of cornea and camera acts as a non-central catadioptric imaging system that requires per-frame calibration through eye pose estimation.

imaging system and, thus, benefit from an extensive theory and literature coverage [115] (**Fig. 5**). Catadioptric systems combine external mirror(s) into the optical path of a camera to achieve particular imaging characteristics. While a perspective camera has a single viewpoint, where all projection rays intersect, catadioptric systems either have a single [6], [14], [79] or multiple viewpoints [117], referred to as central or non-central catadioptric systems, respectively. Calibration denotes the task of determining the projection function, which comprises camera parameters, mirror pose [65], [113] and mirror shape [8], [15], [48]. The cornea, that is shaped similar to an ellipsoid, forms a non-central catadioptric system that requires per-frame calibration through eye pose estimation. For a specular mirror, pose estimation is achieved from its apparent contour and tracked scene correspondences. For the corneal mirror, this may not be possible due to self-occlusion by the eyeball and superimposed iris texture. Methods, therefore, exploit unique eye features and reflections from known light sources.

**Catadioptric stereo system.** A catadioptric system with two or more mirrors captures a scene from different viewpoints. This forms a catadioptric stereo system that allows 3D reconstruction even from a single image [61], [80]. The epipolar geometry, describing the relation of two views in stereo vision, also exists for catadioptric stereo systems. In single viewpoint systems [33], [114], [116], the epipolar plane intersects the surface of the second mirror in a conic section curve that projects to a conic section epipolar curve in the image [116]. In multiple viewpoint systems [115], [117], the epipolar curve is commonly obtained using numerical approaches [136]. Capturing corneal reflections from multiple eye poses creates a non-central catadioptric stereo system. However, regarding the small size of the cornea and the relatively large distance to the camera allows for central approximation with a single focal point at the center of the limbus [83].

## 5.2 Corneal surface reflection

We want to develop a corneal reflection model to calculate the inverse light path towards a point light source, located at an unknown position  $\mathbf{P}$  (**Fig. 6**)<sup>\*4</sup>. Assuming the surface of the cornea to be a perfect mirror, light from position  $\mathbf{P}$  specularly re-

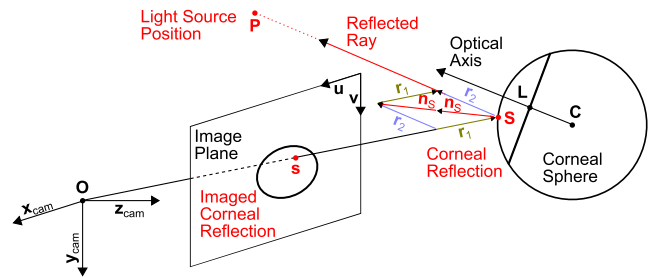


**Fig. 6** Inverse light path towards a point light source. The back-projected light ray from the camera image intersects the corneal surface and reflects into the direction of a light source at an unknown distance from the eye.

flects at surface point  $\mathbf{S}$  into the direction of the camera, where  $\mathbf{S} = (S_x, S_y, S_z)^T$  is described as in

$$\mathbf{S}(\phi, \theta) = \mathbf{C} + r_C \begin{bmatrix} \sin \theta \cos \phi \\ \sin \theta \sin \phi \\ \cos \theta \end{bmatrix}, \quad (4)$$

with the angles of longitude  $\phi \in [0, 2\pi)$  and colatitude  $\theta \in [0, \pi]$ . An image of the eye captures this specular reflection as a bright patch (glint) located within the bounds of the visible iris. Let  $\mathbf{s} = (s_u, s_v, 1)^T$  denote the subpixel location of the patch centroid in the image, and  $\mathbf{S}$  be modeled as ray  $\mathbf{S} = t_1 \mathbf{r}_1$  at an unknown distance  $t_1$  from the camera. Here,  $\mathbf{r}_1 = \mathbf{K}^{-1} \mathbf{s} / \|\mathbf{K}^{-1} \mathbf{s}\|$  is the normalized backprojection vector in the direction of  $\mathbf{S}$ , and  $\mathbf{K}$  the  $3 \times 3$  camera (projection) matrix that contains the intrinsic camera parameters obtained through calibration. To recover  $\mathbf{S}$ , we calculate the intersection with the corneal sphere by solving the quadratic equation  $\|\mathbf{S} - \mathbf{C}\|^2 = r_C^2$  for  $t_1$ . Expanding and re-arranging leads to

$$t_1^2 \mathbf{r}_1^2 - 2t_1 (\mathbf{r}_1 \cdot \mathbf{C}) + \mathbf{C}^2 - r_C^2 = 0 \quad (5)$$

from which we construct the simplified quadratic formula

$$t_1 = (\mathbf{r}_1 \cdot \mathbf{C}) \pm \sqrt{(\mathbf{r}_1 \cdot \mathbf{C})^2 - \mathbf{C}^2 + r_C^2}. \quad (6)$$

<sup>\*4</sup> For this task, it is not necessary to distinguish between an actual source that radiates light and a scene location that reflects incident light from the environment. Thus, we will use both terms interchangeably.

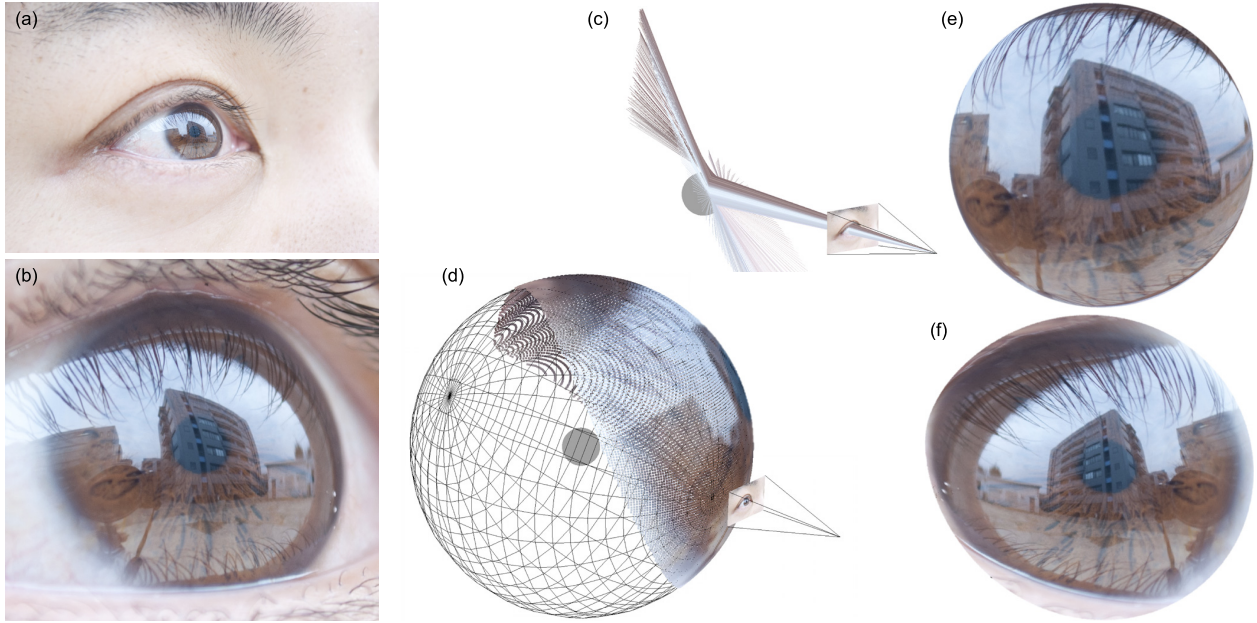


**Fig. 7** Corneal reflection modeling. (a) Eye image ( $3,872 \times 2,592$  pixels) with corneal reflection from an outside environment containing several buildings. (b) Cropped cornea region (approximately  $600 \times 600$  pixels). (c) Back-projection of limbus pixels, intersecting and reflecting at the corneal surface. (d) Environment map (EM): Back-projection of all pixels in the iris region, registered at a sphere around the cornea. (e) EM, outside view towards the cornea. (f) EM, inside view from the cornea.

The first intersection at the front side of the cornea is described by the smaller value of  $t_1$ . Knowing  $\mathbf{S}$  and the corresponding surface normal  $\mathbf{n}_S = (\mathbf{S} - \mathbf{C})/\|\mathbf{S} - \mathbf{C}\|$ , the normalized direction vector  $\mathbf{r}_2$  of the reflection ray is obtained by calculating the specular reflection as in

$$\mathbf{r}_2 = 2(-\mathbf{r}_1 \cdot \mathbf{n}_S)\mathbf{n}_S + \mathbf{r}_1. \quad (7)$$

Light source position  $\mathbf{P}$  then lies on the reflection ray extending from  $\mathbf{S}$ , defined as  $\mathbf{P} = \mathbf{S} + t_2\mathbf{r}_2$ , at an unknown distance  $t_2$ . Registering the reflection rays for the complete iris region at a sphere around the cornea creates a map of environmental illumination (**Fig. 7**).

### 5.3 Light source position estimation

We capture a set of images with varying eye poses for a static point light source. Its unknown position  $\mathbf{P}$  is obtained as the intersection of  $N \geq 2$  inverse reflection rays, by estimating the point with minimal distance to the set of rays (**Fig. 8**).

#### 5.3.1 Geometric approach for $N = 2$

There exists a simple geometric approach for the triangulation of two rays in 3D. The idea is to compute  $\mathbf{P}$  as the midpoint of the shortest line connecting the two rays

$$\begin{aligned} \mathbf{P}_1 &= \mathbf{S}_1 + t_{21}\mathbf{r}_{21}, \\ \mathbf{P}_2 &= \mathbf{S}_2 + t_{22}\mathbf{r}_{22}. \end{aligned} \quad (8)$$

From the orthogonality constraint for the shortest connecting line we obtain the two equations

$$\begin{aligned} (\mathbf{P}_1 - \mathbf{P}_2) \cdot \mathbf{r}_{21} &= 0, \\ (\mathbf{P}_1 - \mathbf{P}_2) \cdot \mathbf{r}_{22} &= 0, \end{aligned} \quad (9)$$

that are solved for  $t_{21}$  and  $t_{22}$ . Inserting the ray Eq. (8) into the

constraints Eq. (9) and expanding the dot product leads to

$$\begin{aligned} (\mathbf{S}_1 - \mathbf{S}_2) \cdot \mathbf{r}_{21} + t_{21}(\mathbf{r}_{21} \cdot \mathbf{r}_{21}) - t_{22}(\mathbf{r}_{22} \cdot \mathbf{r}_{21}) &= 0, \\ (\mathbf{S}_1 - \mathbf{S}_2) \cdot \mathbf{r}_{22} + t_{21}(\mathbf{r}_{21} \cdot \mathbf{r}_{22}) - t_{22}(\mathbf{r}_{22} \cdot \mathbf{r}_{22}) &= 0. \end{aligned} \quad (10)$$

Solving for  $t_{21}$ , back-substituting, and then solving for  $t_{22}$  gives

$$\begin{aligned} t_{21} &= \frac{((\mathbf{S}_1 - \mathbf{S}_2) \cdot \mathbf{r}_{22})(\mathbf{r}_{22} \cdot \mathbf{r}_{21}) - ((\mathbf{S}_1 - \mathbf{S}_2) \cdot \mathbf{r}_{21})(\mathbf{r}_{22} \cdot \mathbf{r}_{22})}{(\mathbf{r}_{21} \cdot \mathbf{r}_{21})(\mathbf{r}_{22} \cdot \mathbf{r}_{22}) - (\mathbf{r}_{22} \cdot \mathbf{r}_{21})(\mathbf{r}_{22} \cdot \mathbf{r}_{21})}, \\ t_{22} &= \frac{((\mathbf{S}_1 - \mathbf{S}_2) \cdot \mathbf{r}_{22}) + t_{21}(\mathbf{r}_{22} \cdot \mathbf{r}_{21})}{(\mathbf{r}_{22} \cdot \mathbf{r}_{22})}. \end{aligned} \quad (11)$$

Finally, the searched point with minimal distance to both rays is obtained as

$$\mathbf{P} = \mathbf{P}_1 + \frac{\mathbf{P}_2 - \mathbf{P}_1}{2}. \quad (12)$$

Note, that when the denominator  $t_{21}$  becomes zero, both rays are parallel and do not intersect. Practically, this case does not occur since different eye poses result in different reflection directions. Nevertheless, it is beneficial to increase the baseline between the cornea positions as this increases the denominator and, thus, the numerical stability.

#### 5.3.2 Algebraic approach for $N \geq 2$

In the general case,  $\mathbf{P}$  can be obtained using matrix algebra as follows: At frame  $l$ , the distance between  $\mathbf{P}$  and the nearest point on the ray  $\mathbf{P}_l = \mathbf{S}_l + t_{2l}\mathbf{r}_{2l}$  is defined as

$$\|\mathbf{P}_l - \mathbf{P}\| = \frac{\|\mathbf{r}_{2l} \times (\mathbf{S}_l - \mathbf{P})\|}{\|\mathbf{r}_{2l}\|}. \quad (13)$$

Knowing  $\|\mathbf{r}_{2l}\| = 1$  and re-arranging leads to

$$\|\mathbf{P}_l - \mathbf{P}\| = \|[\mathbf{r}_{2l}]_{\times} \mathbf{P} - \mathbf{r}_{2l} \times \mathbf{S}_l\|, \quad (14)$$

where  $[\mathbf{r}_{2l}]_{\times}$  represents vector  $\mathbf{r}_{2l}$  as a skew-symmetric matrix,

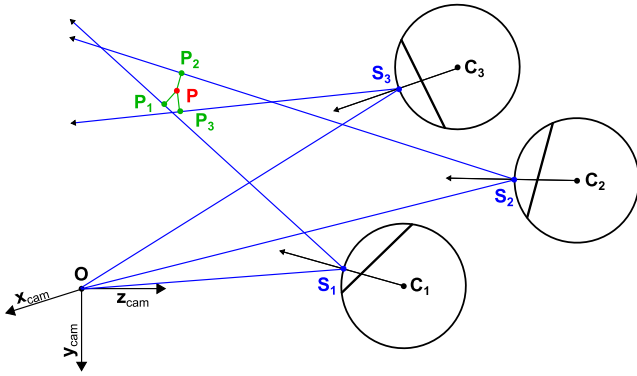


**Fig. 8** Light source position estimation as the intersection of multiple inverse reflection rays. Since the rays generally do not intersect in a single point, we find the least-squares approximation as the point  $\mathbf{P}$  with minimal distance to the set of rays.

given by

$$[\mathbf{r}_{2l}]_{\times} = \begin{bmatrix} 0 & -z_{r_{2l}} & y_{r_{2l}} \\ z_{r_{2l}} & 0 & -x_{r_{2l}} \\ -y_{r_{2l}} & x_{r_{2l}} & 0 \end{bmatrix}, \quad (15)$$

which expresses the cross product as a matrix multiplication. To solve for  $\mathbf{P}$  we combine the  $N$  equations and formulate the problem as a least-squares minimization in the form  $\|\mathbf{A}\mathbf{P} - \mathbf{b}\|$ . Finally, point  $\mathbf{P}$  is estimated, e.g., through the pseudo-inverse as in

$$\mathbf{P} = (\mathbf{A}^T \mathbf{A})^{-1} \mathbf{A}^T \mathbf{b},$$

$$\mathbf{A}_{3N \times 3} = \begin{bmatrix} [\mathbf{r}_{21}]_{\times} \\ \vdots \\ [\mathbf{r}_{2N}]_{\times} \end{bmatrix}, \quad \mathbf{b}_{3N \times 1} = \begin{bmatrix} \mathbf{r}_{21} \times \mathbf{S}_1 \\ \vdots \\ \mathbf{r}_{2N} \times \mathbf{S}_N \end{bmatrix}. \quad (16)$$

#### 5.4 Forward projection

So far, we have covered the back-projection of corneal reflections to estimate the direction and position of light sources. Applications in corneal reflection modeling may also require a solution to the inverse problem of forward-projection from the scene, e.g., to calculate the re-projection error or photometric similarity in estimation, registration and bundle adjustment tasks, which may allow for the combined estimation of eye poses, corneal shape and scene structure. The problem is more difficult since we need to find the point of reflection *without* knowing the direction of the incident light ray. While commonly solved iteratively [34], [115], recent research developed analytic solutions for fast and accurate calculation: Vandepoortaele [125] models the problem for general and quadric-shaped mirrors using polynomials and study their roots. Agrawal et al. [1] provide a comprehensive theory on non-central catadioptric projection. The approach first transforms the problem into the plane of reflection; and then applies the two constraints that (1) the solution lies on the intersection curve with the mirror surface and that (2) the law of reflection requires equal reflection angles and the reflected ray  $\mathbf{r}_2$  to pass through  $\mathbf{P}$ . They show that the solution for quadric-shaped mirrors requires solving a 6th-order polynomial equation. For the special case of a spherical mirror, this reduces to a 4th-order equation that can be solved in closed form. Nitschke [84], and Nakazawa and Nitschke [78] derive another formulation for

a spherical mirror that additionally handles scene locations at an unknown or approximately known distance. The proposed methods enable a novel approach for 3D PoG estimation in arbitrary dynamic environments. For further reading on catadioptric projection, we recommend the extensive survey by Sturm et al. [115].

#### 5.5 Performance evaluation

In the context of display pose reconstruction from corneal reflections, several comprehensive experimental studies analyze the impact of parameter variation in corneal reflection modeling using real [84], [85], [86], [87] and synthetic [84] data. The main factor is the accuracy of surface normals in catadioptric reflection. In line with this, the findings show a large impact of eye pose estimation and individual eye geometry on the overall accuracy. The results from the basic modeling can be considerably improved by optimization, subject to geometric scene constraints using multiple eye poses. Particular achievements from this strategy are a lower reconstruction error with tolerance to noisy measurements and the breaking of an inherent ambiguity in iris-contour based eye pose estimation. Regarding the findings, promising strategies to increase accuracy are, (1) to apply the PCCR concept from active-light to passive eye pose estimation by using scene constraints, (2) to calibrate/estimate individual eye parameters, and (3) to process only reflections near the corneal apex, where the cornea is most spherical.

#### 6. Our work

Previous sections described a first framework for analyzing corneal reflections from multiple eye images that we developed in the context of different projects. The following section provides an overview about our research in the field<sup>\*5</sup>, including motivation, project summaries and general contributions.

**Motivation.** Eye gaze tracking and eye context analysis are important for a large number of applications. However, techniques are still merely research tools in laboratories, operated by professionals with knowledge and experience. It is necessary to develop novel strategies to improve the methods and meet the requirements of the outside world. Corneal reflection analysis provides a direct relationship between the eye and the environment that allows for intriguing applications and novel solution approaches to existing problems. For example, regarding EGT, an application could be PoG tracking in video, where a 3D model of the scene is reconstructed together with camera and eye pose trajectories. Such simultaneous localization and mapping (SLAM) [76] from corneal images could enable unobtrusive interfaces in traditional, ubiquitous and ambient environments. Nevertheless, there is a long way from a first theoretical model of the catadioptric stereo system between two eyes [83] towards a practical strategy for corneal SLAM from multiple eyes, requiring comprehensive knowledge about the geometry of camera, eyes and scene, and solutions to a range of problems. The motivation behind our work is to approach this goal, improve corneal imaging techniques, solve related problems, develop applications and obtain novel insights. With this, we achieve a number of con-

<sup>\*5</sup> <http://www.ime.cmc.osaka-u.ac.jp/~nitschke/Site/Research.html>

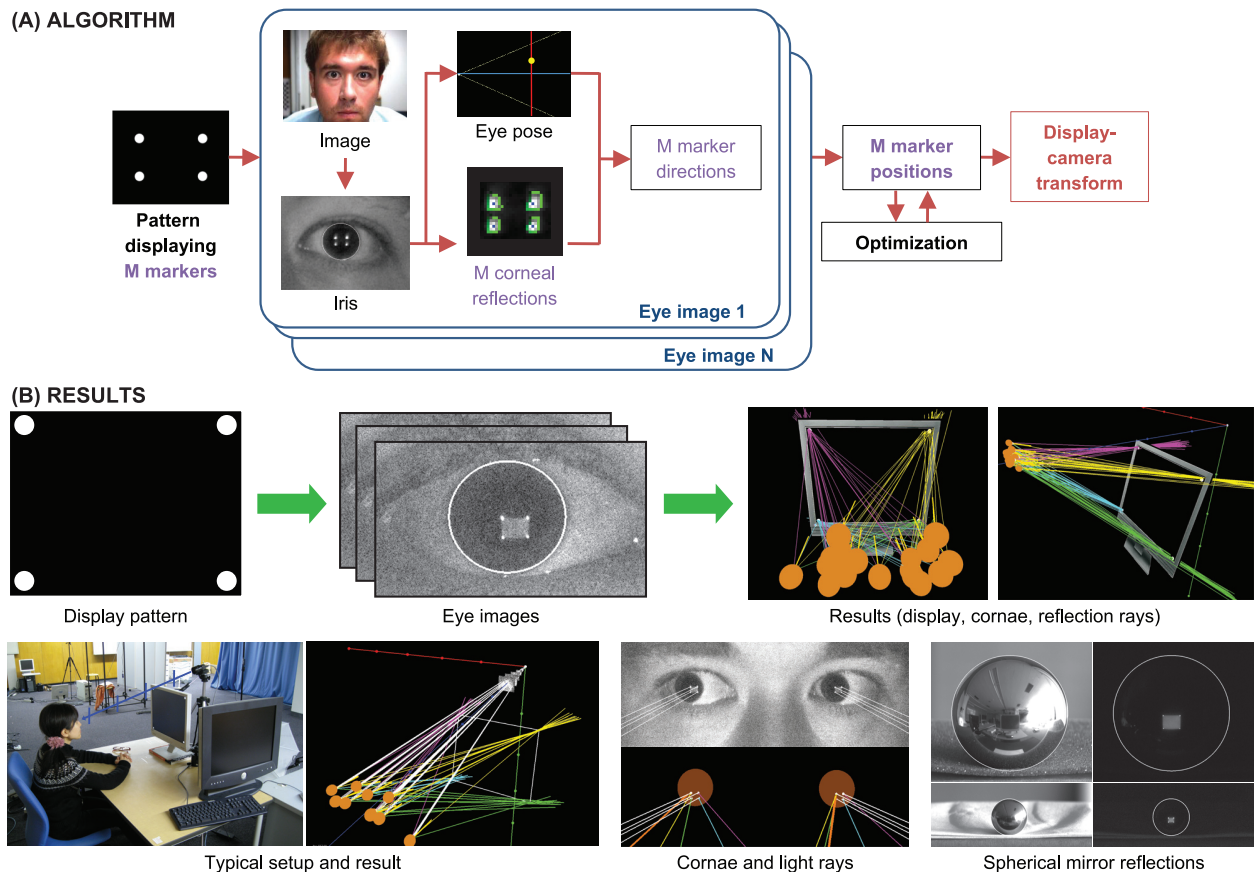


**Fig. 9** Display-camera calibration from eye reflections. (A) Algorithm: The screen shows a pattern with  $M$  circular markers. The corresponding 3D points are reconstructed from the intersections of the  $M$  corneal reflection rays under  $N$  eye poses. (B) Results, showing a typical setup with recovered display, corneal spheres (brown), backprojection (white) and reflection rays (colored).

tributions that may lay the foundation for practical applications and future research in the field.

### 6.1 Display-camera calibration from eye reflections

With advances in vision algorithms, the webcam breaks away from its status of solely being a tool for videoconferencing. Together with a standard monitor or projection screen, this forms a display-camera system that enables a range of interesting vision applications, including active-light object/face reconstruction [19], [30], [100] and vision-based interfaces in HCI [24], [44]. Most applications require a tedious physical calibration to find the pose of the display, commonly achieved by analyzing screen reflections from planar [30] or spherical mirrors [29] at different locations. Motivated by the discovery that screen reflections are clearly visible in eye images, this project [84], [85], [86], [87] develops a novel method that reconstructs the display from at least two eye images (Fig. 9). The method provides several advantages over previous approaches, as it (1) does not require additional hardware, (2) user interaction or awareness, (3) supports dynamic setups, and (4) estimates eye poses for EGT applications. An extension of this work [88] aims to enhance the approach under conditions of practice by encoding display correspondences into illumination patterns for automatic and robust detection.

#### Contributions:

- A thorough experimental evaluation is conducted to evalu-

ate scene reconstruction from corneal reflections using real and synthetic data. The findings provide a tool to assess and improve the accuracy for a particular setup. This is the first study using more than two eye images.

- To compensate for the large error in basic geometric modeling, a non-linear optimization framework is developed that jointly refines multiple eye poses, reflection rays and reconstructed scene, subject to geometric constraints. It allows us to automatically resolve an inherent ambiguity that arises in image-based eye pose estimation (Section 4.2). Several comprehensive experimental studies show that the strategy performs stably with respect to varying subjects, scene poses, eye positions and gaze directions. It also improves results obtained with a spherical mirror. The findings provide general insight in geometric modeling of corneal reflections from multiple eyes and show that constraints can be valuable to improve the results.
- To obtain synthetic data, a framework is developed for physically based rendering of eye images with corneal reflections from environmental illumination [84]. It uses an extended eye model with aspherics, where eye structures are modeled as ellipsoids and cross sections. The framework provides a general tool to simulate the impact of different parameters on scene reconstruction, especially where ground-truth measurements are difficult to obtain, as with parameters related to the individual eye.

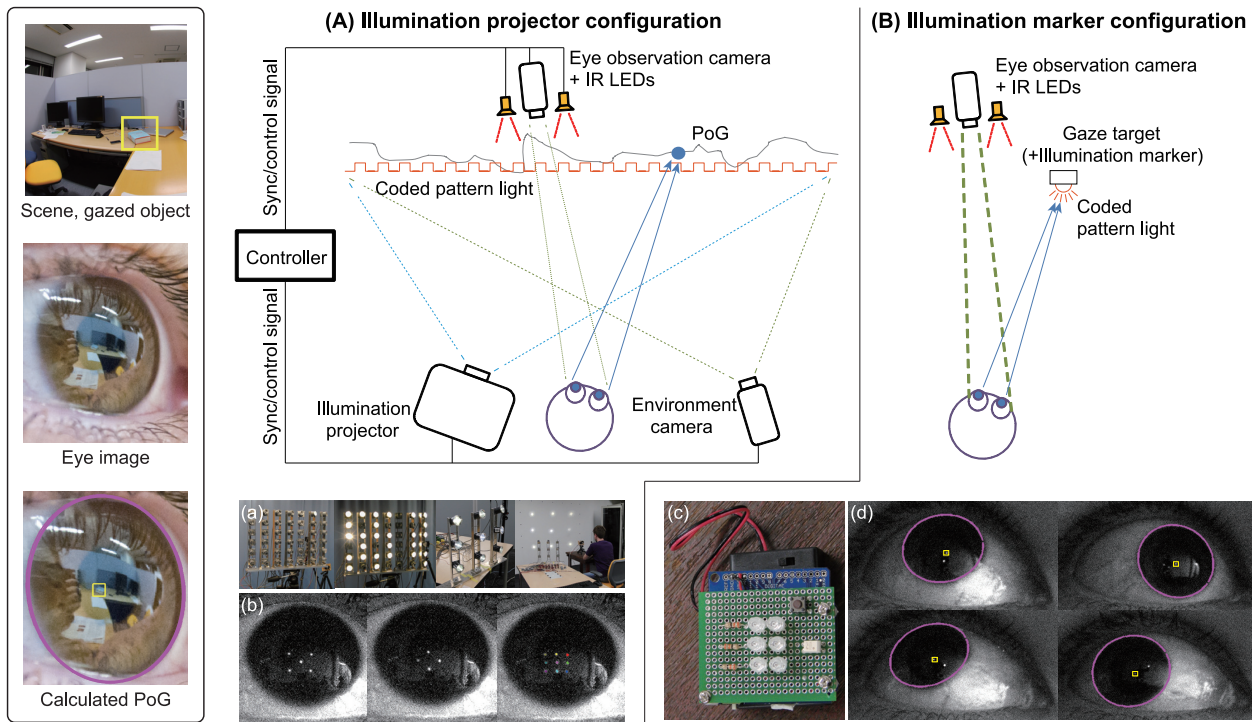


**Fig. 10** Point-of-gaze (PoG) tracking in arbitrary environments. The box on the left summarizes the problem: An environment image shows a book that a person is looking at (yellow square). Corneal reflections of the scene are visible in a corresponding eye image. The algorithm calculates the iris contour (magenta ellipse) and the gaze reflection point (GRP), where light from the PoG is reflected (yellow square). The calculated GRP coincides with the book. (A), (B) Schematic illustration of the approach, where the scene is either illuminated using coded structured light projection (a), (b) or markers (c), (d) that are directly attached to objects.

### 6.2 Point-of-gaze tracking in arbitrary environments

State-of-the-art geometric-eye-modeling-based EGT systems suffer from two major issues: First, mapping the pose of the eye to the PoG requires a tedious *geometric calibration* between eye camera and scene/scene camera, which does not support dynamic setups. Second, due to the fundamental concepts in calculating the PoG by intersecting the gaze ray with a scene model, systems potentially suffer from a *parallax issue* under depth-varying conditions (as in complex scene geometry or mobile systems). This explains the common restriction to simple target scenes like computer screens and walls. This project [78], [84] develops a novel PoG estimation approach that overcomes the issues through a *direct mapping* between corneal images and the scene (Fig. 10).

#### Contributions:

- Direct correspondence matching in corneal and scene images establishes a calibration-free relationship between the eye and the scene and, therefore, naturally supports dynamic configurations and depth-varying environments (with remote and head-mounted systems). High accuracy is achieved as the matching does not depend on geometric calculations. This is a novel fundamental concept in EGT. Moreover, it enables the computation of eye related information from conventional images with much higher quality.
- Active coded illumination allows for robust correspondence matching by assigning scene locations with coded patterns that can be identified from within both, corneal and scene images, which is difficult to achieve with passively captured images. Experimental results verify the robustness under

challenging conditions, such as short exposure, image noise, environmental light and dense matching. This is the first application of coded structured light in the context of eye imaging and corneal reflection analysis. Imperceptible (high-frequency complement patterns) or invisible (IR) structured light [28] is not perceived by human observers; and imperceptible codes can be removed from images to recover the texture of the scene. The concept is verified by two prototype implementations with specially-designed hardware. One uses an IR-LED array projector that allows for non-intrusive, dense and wide-angle illumination (Fig. 10 (A)). The other uses small IR-LED illumination devices that are directly attached onto gaze target objects and allow for simple setups without a scene camera (Fig. 10 (B)).

- An analytic solution is developed for the forward projection problem, where the projected scene point is defined up to an unknown distance from the mirror along a particular direction. The developed solution becomes necessary as the method of Agrawal et al. [1] is not applicable in this more general case. The strategy is applied to obtain the GRP, where light from the PoG in the scene reflects at the corneal surface into an eye image. A simple one-point calibration increases the accuracy to the level of state-of-the-art EGT systems by compensating for the individual offset between optical and visual axis.

### 6.3 Super-resolution from corneal images

Corneal reflection modeling enables a large number of appli-

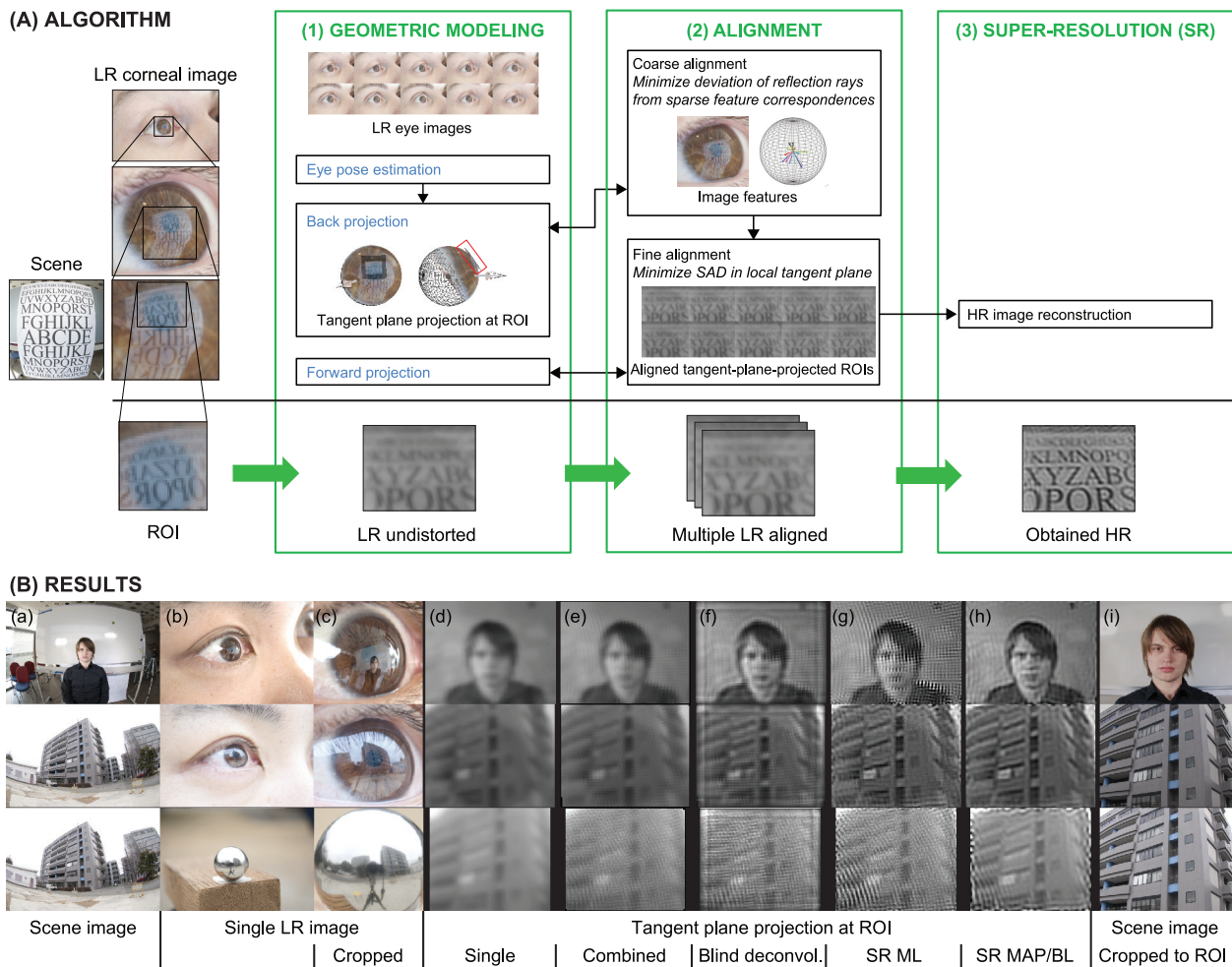


**Fig. 11** Super-resolution from corneal images. (A) The algorithm involves a three-step approach comprising (1) eye pose estimation and calculation of LR environment maps, (2) registration of multiple maps and optimization of system parameters, and (3) reconstruction of an HR image. (B) SR result for different scenes (from 10 LR images). (a) Scene image. (b) Single LR image. (c) Cropped. (d)–(h) Environment map local plane projection at region of interest (ROI): (d) Single LR image. (e) Combined aligned LR images. (f) Blind deconvolution of (e). (g), (h) SR result: (g) Maximum-likelihood (ML). (h) Maximum a posteriori (MAP) with bilateral filter residual prior (BL) [122]. (k) Scene image, cropped to ROI. The bottom row shows results from a spherical mirror at the size of the human cornea.

cations. In reality, however, even if we manually capture images with a high-resolution camera that is placed near the eye and carefully adjusted to avoid motion and defocus blur, the quality of corneal reflections is largely limited. To simplify the acquisition of corneal images, this work [89] develops a super-resolution (SR) [119] strategy that reconstructs a high-resolution (HR) scene image from a series of lower resolution (LR) corneal images, such as occurring in surveillance or personal videos (Fig. 11 (A)). Analytic forward projection allows to efficiently handle the large number of re-projections in registration. A number of experiments for indoor and outdoor scenes confirm that the strategy recovers high-frequency textures (with a quality high enough to recognize small characters, human faces and fine structures) that are lost in the source images (Fig. 11 (B)).

**Contributions:**

- The strategy works with spherical mirrors, suggesting applicability to other non-central catadioptric systems such as specular and liquid surfaces. This is also the first SR approach for non-central catadioptric systems.

- Since the technique solves the quality degradation problem in corneal imaging, it may become a foundation for future research in the field. The obtained information about a person and the environment has the potential to enable novel applications, e.g., for surveillance systems, personal video, human-computer interaction and upcoming head-mounted cameras (Google Glass) [35].

**7. Implications**

The described techniques for geometric modeling of corneal reflections from multiple eye images obtain rich information that can remove the need for artificial environments, expert supervision, subject awareness, and complex hardware and setup procedures, which enables novel approaches in visual eye analysis. A major point is the obtained relationship between cameras, eyes and scene, that removes the need for external calibration. This allows for dynamic scenarios, such as in user tracking, mobile systems and human-altered environments, and scenarios that do not allow for a dedicated calibration—because of time, ability or

awareness constraints. We believe that geometric eye and corneal reflection modeling has the potential to facilitate a wide range of applications and want to discuss implications for different fields.

**Visual recognition.** The environment map from a corneal image provides information about the location and situation in which a person was photographed. Integrating multiple eye and scene images can increase the quality of the results. This allows for data exploration in surveillance, eavesdropping [5] and forensics [51], and provides context information in face/body analysis and scene understanding.

**Computer graphics and vision.** The obtained environment map further describes incident illumination, which allows recovery of scene structure and reflectance. This enables a large number of applications, such as scene relighting [82], [123], illumination normalization in object, face and iris recognition [22], [81], and illumination consistency analysis in digital forgery detection [51]. On the other hand, known scene structure and illumination provide constraints in eye modeling to improve imaged eye features through corneal reflection removal and refraction correction.

**Human-computer interaction (HCI).** Eye analysis is traditionally applied to the gaze-based interaction with controlled planar screens [12]. Geometric modeling, however, provides additional information and flexibility that can enable intelligent sensors for ubiquitous and ambient applications, integrated with off-the-shelf products to be used under conditions of practice. Applying anthropometric knowledge permits tracking the complete perceived field-of-view of a person, instead of only the PoG. The support of arbitrary environments allows to study human behavior in human intent analysis, robot teaching, algorithm design and human factors engineering. Especially children and infants benefit from remote operation through the absence of obtrusive body-attachments. Eye gaze tracking is a common task with a long history [24], [44], [140], relevant to a large number of applications in a variety of fields [23]. Nevertheless, there still remain several issues that need to be solved.

**Diagnostic studies.** Capturing a person's eyes and face in the same image allows us to analyze the gazed scene together with the person's reaction [72]. Such stimulus-response information enables diagnostic studies in many disciplines, including medicine, psychology, engineering and marketing. Specifically, this can help to diagnose degrading of the visual and motor systems, analyze human factors, or understand the human mind, attraction, problem solving, communication, interaction and social networks. Geometric modeling provides additional benefits compared to traditional eye analysis: (1) Remote visual inspection facilitates non-intrusive methods, where equipment and conditions do not interfere with the task or otherwise affect the subject. (2) The absence of geometric calibration allows for interactive studies and unknown conditions that can provide novel insights. (3) Correspondence matching between corneal reflections and direct views provides high quality scene information for further processing.

## 8. Future directions

This paper has shown that geometric eye and corneal reflection

modeling has the potential to facilitate novel applications. Nevertheless, we discussed that, while actual solutions can benefit from theories and techniques in catadioptric imaging [115], they demand for specialized algorithms that handle the unique properties of the eye. With our work, we exploit corneal imaging to introduce novel applications and approaches for solving persisting problems in other domains. Beside this, we obtain novel insights and achieve a number of general contributions that make corneal imaging more practicable and may lay the foundation for future research in the field. Nevertheless, there still remains tremendous requirement for improvement in the underlying techniques to support non-professional scenarios and arbitrary environments under conditions of practice. Let us now discuss promising future directions, covering improved methods, novel problem solutions and interesting applications. As the described ideas apply to different stages of the algorithmic pipeline, they may as well be combined.

**Correspondence matching** refers to matching eye features, or direct and reflected scene features among multiple eye and scene images. (1) Eye features are anatomic point, contour or texture features, of the eyeball or the occluding contour of the skin, related to the pupil, iris, sclera, eye lids or eye corners. Pupil and iris features require handling of refraction, which depends on the shape of the cornea. While commonly assumed spherical, an accurate model of corneal shape may be reconstructed by modeling scene reflections or iris texture refraction. Tracking iris texture features may further allow for corneal reflection segmentation and eye pose estimation, but implies high resolution and high quality images. (2) Matching direct and reflected scene features in passively captured images requires handling the geometric distortion from the corneal shape, the photometric distortion from the iris texture, and the reduced intensity and dynamic range from the low reflectivity of the cornea. Solving the described issues relates corneal reflections with high quality scene information that may allow for reflection removal, eye pose and shape estimation, and visualization of a person's field-of-view. Another important application is PoG tracking in arbitrary (non-planar) environments, *without* using active coded illumination as described in Section 6.2 [78]. A possible scenario is combined EGT and structure-from-motion (SfM), either with a hand-held or surveillance video camera.

**Coded illumination** enables the optical transmission of information. This has been widely used to identify environment locations, either for scene reconstruction by structured light using projectors [99] and monitors [8], [48], or for object tagging using projectors [141] and LEDs [108]. Therefore, coded illumination may be applied to the accurate and robust correspondence matching over any combination of eye and scene images. Particular advantages include its robustness compared to natural feature tracking and epipolar geometry, and its support for dense matching over a wide area. Non-intrusiveness is achieved by exploiting invisible (IR) light or the imperceptibility of complement patterns at high framerates [28]. For more information on the topic, refer to Refs. [78], [84], [88]. Special LED arrays have been applied in EGT to allow for automatic reflection extraction and increased robustness [47], [67]. While termed as "structured light," this relates only to the geometric alignment, not the encoding of light.

**Scene constraints** can be assigned to tracked features to solve for unknown information or increase accuracy. Well suited are geometric constraints from 3D points, lines and planes that commonly occur in human-made environments. Standard PCCR methods in EGT apply point features (glints) from known light sources for eye pose estimation [37], [106]. The approach may be extended to the illumination from an unknown environment, where structure information may be obtained using stereo or SfM. A 3D line, imaged by a catadioptric system, allows recovering the line, as well as the pose and shape of an axisymmetric mirror [31], [62]. Combining constraints from lines and planes enables recovering planar polygonal light sources [102]. Line and plane constraints are less common in corneal reflection analysis, and have been exploited only for display pose estimation and EGT [87], [101]. Nevertheless, there exists a wide range of literature in catadioptric imaging, regarding the recovery of mirror pose, shape and scene geometry [115]. Finally, all measurements may be integrated into a bundle-adjustment framework to obtain and optimize unknown parameters, probably in conjunction with outlier removal.

**Eye information.** Eye pose and shape estimation using correspondence matches or scene constraints has been largely discussed. In case an environment map is available, a different strategy similar to Ref. [16] may be applied, where an actual eye image is matched against a database of specular highlight or flow images, rendered offline for varying eye poses and shapes. Nearly all methods in geometric eye modeling assume the cornea to be spherical. However, as the eyeball is slightly flattened in the vertical plane [109], and the corneal topology is complex [11], [32], it is necessary to develop strategies for parameterizing and calibrating more accurate models. Existing aspherical approaches assume an axisymmetric shape and require known light sources [77] or geometric constraints [31]. Further improvements may be achieved with more general parametric models, which are calibrated using scene constraints or image matching. Finally, an interesting direction in eye analysis is to develop solutions that combine low-cost optical hardware with personal devices to enable self-assessment of visual conditions, such as refractive errors, focal range, focusing speed and lens opacity [92], [93]. The results may also be used to correct the visual content in digital devices.

## 9. Conclusion

This paper provided an overview on the geometric analysis of corneal reflections to relate the individual (eye) with the physical world, which creates a flexible non-intrusive framework for tracking cameras, eyes and visual scene information to solve various problems<sup>\*6</sup>. Besides this, the study serves a number of objectives to support advancement of the state-of-the-art. Particular contributions include a motivation for the topic, a characterization of its relation to different fields, an introduction to the anatomic background, a technical description of geometric eye and reflection modeling, and a discussion of our work, implications and future directions.

<sup>\*6</sup> The interested reader may refer to Ref. [84] for an in-depth coverage of the topic.

We explained the relevance to a number of fields, including visual recognition, computer graphics and vision, human-computer interaction and diagnostic studies. Advancement in computational systems, devices and architectures demands for novel interfaces and forms of interaction. In this context, the established link between the eye and the environment allows for a combined analysis of stimulus and interaction that may lead to novel insights when analyzed with data mining techniques.

Nevertheless, practical solutions require handling a number of persisting technical problems, to achieve the ultimate goal of modeling the scene structure and illumination distribution, using multiple eye and scene images, under dynamic camera and eye poses. We identified promising future directions regarding improved methods, novel problem solutions and interesting applications, focusing on the topics of feature correspondence matching, coded illumination, scene constraints and eye-related information.

**Acknowledgments** This work was supported by the JST PRESTO program.

## References

- [1] Agrawal, A., Taguchi, Y. and Ramalingam, S.: Beyond Alhazen's problem: Analytical projection model for non-central catadioptric cameras with quadric mirrors, *Proc. IEEE Conference on Computer Vision and Pattern Recognition (CVPR)*, pp.2993–3000 (2011).
- [2] Agustin, J.S., Villanueva, A. and Cabeza, R.: Pupil brightness variation as a function of gaze direction, *Proc. ACM Symposium on Eye Tracking Research & Applications (ETRA)*, p.49 (2006).
- [3] Arvacheh, E.M. and Tizhoosh, H.R.: IRIS Segmentation: Detecting Pupil, Limbus and Eyelids, *Proc. IEEE International Conference on Image Processing (ICIP)*, pp.2453–2456 (2006).
- [4] Atchison, D.A. and Smith, G.: *Optics of the Human Eye*, Butterworth-Heinemann, Edinburgh (2000).
- [5] Backes, M., Chen, T., Dürmuth, M., Lensch, H.P.A. and Welk, M.: Tempest in a Teapot: Compromising Reflections Revisited, *Proc. IEEE Symposium on Security and Privacy (SP)*, pp.315–327 (2009).
- [6] Baker, S. and Nayar, S.K.: A Theory of Single-Viewpoint Catadioptric Image Formation, *Int. J. Comput. Vision*, Vol.35, No.2, pp.175–196 (1999).
- [7] Baker, T.Y.: Ray tracing through non-spherical surfaces, *Proc. Phys. Soc.*, Vol.55, No.5, pp.361–364 (1943).
- [8] Balzer, J. and Werling, S.: Principles of Shape from Specular Reflection, *Measurement*, Vol.43, No.10, pp.1305–1317 (2010).
- [9] Barry, J.C., Pongs, U.M. and Hillen, W.: Algorithm for Purkinje images I and IV and limbus centre localization, *Comput. Biol. Med.*, Vol.27, No.6, pp.515–531 (1997).
- [10] Beymer, D. and Flickner, M.: Eye gaze tracking using an active stereo head, *Proc. IEEE Conference on Computer Vision and Pattern Recognition (CVPR)*, pp.451–458 (2003).
- [11] Bogan, S.J., Waring III, G.O., Ibrahim, O., Drews, C. and Curtis, L.: Classification of Normal Corneal Topography Based on Computer-Assisted Videokeratography, *Arch. Ophthalmol.*, Vol.108, No.7, pp.945–949 (1990).
- [12] Bolt, R.A.: Eyes at the interface, *Proc. ACM Conference on Human Factors in Computing Systems (CHI)*, pp.360–362 (1982).
- [13] Bowyer, K.W., Hollingsworth, K. and Flynn, P.J.: Image understanding for iris biometrics: A survey, *Comput. Vis. Image Underst.*, Vol.110, No.2, pp.281–307 (2008).
- [14] Bruckstein, A.M. and Richardson, T.J.: Omniview Cameras with Curved Surface Mirrors, *Proc. IEEE Workshop on Omnidirectional Vision (OMNIVIS)*, pp.79–84 (2000).
- [15] Caglioti, V., Taddei, P., Boracchi, G., Gasparini, S. and Giusti, A.: Single-Image Calibration of Off-Axis Catadioptric Cameras Using Lines, *Proc. IEEE International Conference on Computer Vision (ICCV)*, pp.1–6 (2007).
- [16] Chang, J.Y., Raskar, R. and Agrawal, A.: 3D pose estimation and segmentation using specular cues, *Proc. IEEE Conference on Computer Vision and Pattern Recognition (CVPR)*, pp.1706–1713 (2009).
- [17] Chen, J. and Ji, Q.: 3D Gaze Estimation with a Single Camera without IR Illumination, *Proc. IEEE International Conference on Pattern Recognition (ICPR)*, pp.1–4 (2008).

- [18] Chen, Q., Wu, H. and Wada, T.: Camera Calibration with Two Arbitrary Coplanar Circles, *Proc. European Conference on Computer Vision (ECCV)*, pp.521–532 (2004).
- [19] Clark, J.J.: Photometric stereo using LCD displays, *Image Vision Comput.*, Vol.28, No.4, pp.704–714 (2010).
- [20] Colombo, C., Comanducci, D. and Bimbo, A.D.: Robust tracking and remapping of eye appearance with passive computer vision, *ACM Trans. Multimedia Comput. Commun. Appl.*, Vol.3, No.4, pp.2:1–2:20 (2007).
- [21] Crick, R.P. and Khaw, P.T.: *A Textbook of Clinical Ophthalmology*, World Scientific, Singapore, 3rd edition (2003).
- [22] Daugman, J.: How iris recognition works, *IEEE Trans. Circuits Syst. Video Technol.*, Vol.14, No.1, pp.21–30 (2004).
- [23] Duchowski, A.T.: A breadth-first survey of eye-tracking applications, *Behav. Res. Meth. Instrum. Comput.*, Vol.34, No.4, pp.455–470 (2002).
- [24] Duchowski, A.T.: *Eye Tracking Methodology: Theory and Practice*, Springer-Verlag London, Ltd., 2nd edition (2007).
- [25] Ebisawa, Y.: Improved video-based eye-gaze detection method, *IEEE Trans. Instrum. Meas.*, Vol.47, No.4, pp.948–955 (1998).
- [26] Escudero-Sanz, I. and Navarro, R.: Off-axis aberrations of a wide-angle schematic eye model, *J. Opt. Soc. Am. A*, Vol.16, No.8, pp.1881–1891 (1999).
- [27] Fitzgibbon, A., Pilu, M. and Fisher, R.B.: Direct least square fitting of ellipses, *IEEE Trans. Pattern Anal. Mach. Intell.*, Vol.21, No.5, pp.476–480 (1999).
- [28] Fofi, D., Sliwa, T. and Voisin, Y.: A comparative survey on invisible structured light, *Proc. SPIE 5303 Machine Vision Applications in Industrial Inspection XII*, pp.90–98 (2004).
- [29] Francken, Y., Hermans, C. and Bekaert, P.: Screen-Camera Calibration using Gray Codes, *Proc. IEEE Canadian Conference on Computer and Robot Vision (CRV)*, pp.155–161 (2009).
- [30] Funk, N. and Yang, Y.-H.: Using a Raster Display for Photometric Stereo, *Proc. IEEE Canadian Conference on Computer and Robot Vision (CRV)*, pp.201–207 (2007).
- [31] Gasparini, S. and Caglioti, V.: Line Localization from Single Catadioptric Images, *Int. J. Comput. Vision*, Vol.94, pp.361–374 (2011).
- [32] Gatinel, D., Malet, J., Hoang-Xuan, T. and Azar, D.T.: Corneal Elevation Topography: Best Fit Sphere, Elevation Distance, Asphericity, Toricity, and Clinical Implications, *Cornea*, Vol.30, No.5, pp.508–515 (2011).
- [33] Geyer, C. and Daniilidis, K.: Properties of the Catadioptric Fundamental Matrix, *Proc. European Conference on Computer Vision (ECCV)*, pp.536–538 (2002).
- [34] Goncalves, N. and Araujo, H.: Projection Model, 3D Reconstruction and Rigid Motion Estimation from Non-Central Catadioptric Images, *Proc. International Symposium on 3D Data Processing, Visualization and Transmission (3DPVT)*, pp.325–332 (2004).
- [35] Google: Project Glass on Google+, available from (<http://plus.google.com/+projectglass/>) (accessed 2012-09-30).
- [36] Grabowski, K., Sankowski, W., Zubert, M. and Napieralska, M.: Reliable iris localization method with application to iris recognition in near infrared light, *Proc. IEEE International Conference on Mixed Design of Integrated Circuits and System (MIXDES)*, pp.684–687 (2006).
- [37] Guestrin, E.D. and Eizenman, M.: General Theory of Remote Gaze Estimation Using the Pupil Center and Corneal Reflections, *IEEE Trans. Biomed. Eng.*, Vol.53, No.6, pp.1124–1133 (2006).
- [38] Guestrin, E.D. and Eizenman, M.: Remote point-of-gaze estimation with single-point personal calibration based on the pupil boundary and corneal reflections, *Proc. IEEE Canadian Conference on Electrical and Computer Engineering (CCECE)*, pp.000971–000976 (2011).
- [39] Gullstrand, A.: *Helmholtz's Handbuch der Physiologischen Optik*, Vol.1, chapter Appendices II and IV, pp.301–358, 382–415, Voss Hamburg (1909).
- [40] Gurdjos, P., Sturm, P. and Wu, Y.: Euclidean Structure from  $N \geq 2$  Parallel Circles: Theory and Algorithms, *Proc. European Conference on Computer Vision (ECCV)*, pp.238–252 (2006).
- [41] Halir, R. and Flusser, J.: Numerically Stable Direct Least Squares Fitting of Ellipses, *Proc. International Conference in Central Europe on Computer Graphics and Visualization (WSCG)*, pp.125–132 (1998).
- [42] Halstead, M.A., Barsky, B.A., Klein, S.A. and Mandell, R.B.: Reconstructing curved surfaces from specular reflection patterns using spline surface fitting of normals, *Proc. ACM SIGGRAPH*, pp.335–342 (1996).
- [43] Hansen, D.W., Agustin, J.S. and Villanueva, A.: Homography normalization for robust gaze estimation in uncalibrated setups, *Proc. ACM Symposium on Eye Tracking Research & Applications (ETRA)*, pp.13–20 (2010).
- [44] Hansen, D.W. and Ji, Q.: In the eye of the beholder: A survey of models for eyes and gaze, *IEEE Trans. Pattern Anal. Mach. Intell.*, Vol.32, No.3, pp.478–500 (2010).
- [45] Hartley, R. and Zisserman, A.: *Multiple View Geometry in Computer Vision*, Cambridge University Press, New York, NY, 2nd edition (2003).
- [46] Hennessey, C., Nouredin, B. and Lawrence, P.: A single camera eye-gaze tracking system with free head motion, *Proc. ACM Symposium on Eye Tracking Research & Applications (ETRA)*, pp.87–94 (2006).
- [47] Hua, H., Krishnaswamy, P. and Rolland, J.P.: Video-based eyetracking methods and algorithms in head-mounted displays, *Opt. Express*, Vol.14, No.10, pp.4328–4350 (2006).
- [48] Ihrke, I., Kutulakos, K.N., Lensch, H.P.A., Magnor, M.A. and Heidrich, W.: Transparent and Specular Object Reconstruction, *Comput. Graph. Forum*, Vol.29, No.8, pp.2400–2426 (2010).
- [49] Iskander, D.R., Collins, M.J., Mioschek, S. and Trunk, M.: Automatic pupillometry from digital images, *IEEE Trans. Biomed. Eng.*, Vol.51, No.9, pp.1619–1627 (2004).
- [50] Iskander, D.: A parametric approach to measuring limbus corneae from digital images, *IEEE Trans. Biomed. Eng.*, Vol.53, No.6, pp.1134–1140 (2006).
- [51] Johnson, M.K. and Farid, H.: Exposing Digital Forgeries Through Specular Highlights on the Eye, *Proc. International Workshop on Information Hiding (IH)*, pp.311–325 (2007).
- [52] Kanatani, K. and Liu, W.: 3D interpretation of conics and orthogonality, *CVGIP Image Underst.*, Vol.58, No.3, pp.286–301 (1993).
- [53] Kang, J.J., Eizenman, M., Guestrin, E.D. and Eizenman, E.: Investigation of the Cross-Ratios Method for Point-of-Gaze Estimation, *IEEE Trans. Biomed. Eng.*, Vol.55, No.9, pp.2293–2302 (2008).
- [54] Kaufman, P.L. and Alm, A.: *Adler's Physiology of the Eye: Clinical Application*, Mosby, Inc., St. Louis, MO, 10th edition (2003).
- [55] Khurana, A.K.: *Comprehensive Ophthalmology*, New Age International (P) Ltd., New Delhi, 4th edition (2007).
- [56] Kim, S.M., Sked, M. and Ji, Q.: Non-intrusive eye gaze tracking under natural head movements, *Proc. International Conference of the IEEE Engineering in Medicine and Biology Society (EMBS)*, pp.2271–2274 (2004).
- [57] Kohlbecher, S., Bardinst, S., Bartl, K., Schneider, E., Poitschke, T. and Ablassmeier, M.: Calibration-free eye tracking by reconstruction of the pupil ellipse in 3D space, *Proc. ACM Symposium on Eye Tracking Research & Applications (ETRA)*, pp.135–138 (2008).
- [58] Kooijman, A.C.: Light distribution on the retina of a wide-angle theoretical eye, *J. Opt. Soc. Am.*, Vol.73, No.11, pp.1544–1550 (1983).
- [59] Lam, M.W.Y. and Baranoski, G.V.G.: A Predictive Light Transport Model for the Human Iris, *Comput. Graph. Forum*, Vol.25, No.3, pp.359–368 (2006).
- [60] Lambooi, M., IJsselstein, W., Fortuin, M. and Heynderickx, I.: Visual Discomfort and Visual Fatigue of Stereoscopic Displays: A Review, *Journal of Imaging Science and Technology*, Vol.53, No.3, pp.1–14 (2009).
- [61] Lanman, D., Crispell, D., Wachs, M. and Taubin, G.: Spherical Catadioptric Arrays: Construction, Multi-View Geometry, and Calibration, *Proc. International Symposium on 3D Data Processing, Visualization, and Transmission (3DPVT)*, pp.81–88 (2006).
- [62] Lanman, D., Wachs, M., Taubin, G. and Cukierman, F.: Reconstructing a 3D Line from a Single Catadioptric Image, *Proc. International Symposium on 3D Data Processing, Visualization, and Transmission (3DPVT)*, pp.89–96 (2006).
- [63] Le Grand, Y. and El Hage, S.G.: *Physiological Optics*, Springer Berlin (1980).
- [64] Lefohn, A., Budge, B., Shirley, P., Caruso, R. and Reinhard, E.: An Ocularist's Approach to Human Iris Synthesis, *IEEE Comput. Graphics Appl.*, Vol.23, No.6, pp.70–75 (2003).
- [65] Lhuillier, M.: Automatic scene structure and camera motion using a catadioptric system, *Comput. Vis. Image Underst.*, Vol.109, No.2, pp.186–203 (2008).
- [66] Li, D., Winfield, D. and Parkhurst, D.J.: Starburst: A hybrid algorithm for video-based eye tracking combining feature-based and model-based approaches, *Proc. IEEE Conference on Computer Vision and Pattern Recognition Workshops (CVPRW)*, pp.79–86 (2005).
- [67] Li, F., Kolakowski, S. and Pelz, J.: Using Structured Illumination to Enhance Video-Based Eye Tracking, *Proc. IEEE International Conference on Image Processing (ICIP)*, pp.373–376 (2007).
- [68] Liou, H.L. and Brennan, N.A.: Anatomically accurate, finite model eye for optical modeling, *J. Opt. Soc. Am. A*, Vol.14, No.8, pp.1684–1695 (1997).
- [69] Lotmar, W.: Theoretical Eye Model with Aspherics, *J. Opt. Soc. Am.*, Vol.61, No.11, pp.1522–1529 (1971).
- [70] Mandell, R.B.: A guide to videokeratography, *Int. Contact Lens*

- Clin.*, Vol.23, No.6, pp.205–228 (1996).
- [71] Matey, J.R., Broussard, R. and Kennell, L.: Iris image segmentation and sub-optimal images, *Image Vision Comput.*, Vol.28, No.2, pp.215–222 (2010).
- [72] Matsumoto, D., Keltner, D., Shiota, M.N., O’Sullivan, M. and Frank, M.: *Facial Expressions of Emotion*, chapter Facial expressions of emotion, pp.211–234, Guilford Press New York, NY, 3rd edition (2008).
- [73] Merchant, J., Morrisette, R. and Porterfield, J.L.: Remote measurement of eye direction allowing subject motion over one cubic foot of space, *IEEE Trans. Biomed. Eng.*, Vol.21, No.4, pp.309–317 (1974).
- [74] Morimoto, C.H., Koons, D., Amir, A. and Flickner, M.: Pupil detection and tracking using multiple light sources, *Image Vision Comput.*, Vol.18, No.4, pp.331–335 (2000).
- [75] Morimoto, C.H. and Mimica, M.R.M.: Eye gaze tracking techniques for interactive applications, *Comput. Vis. Image Underst.*, Vol.98, No.1, pp.4–24 (2005).
- [76] Muhammad, N., Fofi, D. and Ainouz, S.: Current state of the art of vision based SLAM, *Proc. SPIE Image Processing: Machine Vision Applications II*, Vol.7251, No.1, p.72510F (2009).
- [77] Nagamatsu, T., Iwamoto, Y., Kamahara, J., Tanaka, N. and Yamamoto, M.: Gaze estimation method based on an aspherical model of the cornea: surface of revolution about the optical axis of the eye, *Proc. ACM Symposium on Eye Tracking Research & Applications (ETRA)*, pp.255–258 (2010).
- [78] Nakazawa, A. and Nitschke, C.: Point of Gaze Estimation through Corneal Surface Reflection in an Active Illumination Environment, *Proc. 12th European Conference on Computer Vision (ECCV)*, Fitzgibbon et al. (Ed.), LNCS, Vol.7573, Springer Berlin/Heidelberg, pp.159–172 (2012).
- [79] Nayar, S.K. and Peri, V.: Folded Catadioptric Cameras, *Proc. IEEE Conference on Computer Vision and Pattern Recognition (CVPR)*, pp.217–223 (1999).
- [80] Nene, S.A. and Nayar, S.K.: Stereo with Mirrors, *Proc. IEEE International Conference on Computer Vision (ICCV)*, pp.1087–1094 (1998).
- [81] Nishino, K., Belhumeur, P.N. and Nayar, S.K.: Using Eye Reflections for Face Recognition Under Varying Illumination, *Proc. IEEE International Conference on Computer Vision (ICCV)*, pp.519–526 (2005).
- [82] Nishino, K. and Nayar, S.K.: Eyes for Relighting, *Proc. ACM SIGGRAPH*, pp.704–711 (2004).
- [83] Nishino, K. and Nayar, S.K.: Corneal Imaging System: Environment from Eyes, *Int. J. Comput. Vision*, Vol.70, No.1, pp.23–40 (2006).
- [84] Nitschke, C.: Image-based Eye Pose and Reflection Analysis for Advanced Interaction Techniques and Scene Understanding, PhD Thesis, Graduate School of Information Science and Technology, Osaka University (2011).
- [85] Nitschke, C., Nakazawa, A. and Takemura, H.: Display-camera calibration from eye reflections, *Proc. IEEE International Conference on Computer Vision (ICCV)*, pp.1226–1233 (2009).
- [86] Nitschke, C., Nakazawa, A. and Takemura, H.: Eye reflection analysis and application to display-camera calibration, *Proc. IEEE International Conference on Image Processing (ICIP)*, pp.3449–3452 (2009).
- [87] Nitschke, C., Nakazawa, A. and Takemura, H.: Display-camera calibration using eye reflections and geometry constraints, *Comput. Vis. Image Underst.*, Vol.115, No.6, pp.835–853 (2011).
- [88] Nitschke, C., Nakazawa, A. and Takemura, H.: Practical Display-Camera Calibration from Eye Reflections using Coded Illumination, *Proc. IEEE Asian Conference on Pattern Recognition (ACPR)*, pp.550–554 (2011).
- [89] Nitschke, C. and Nakazawa, A.: Super-Resolution from Corneal Images, *Proc. British Machine Vision Conference (BMVC)*, pp.1–12 (2012).
- [90] Ohno, T., Mukawa, N. and Yoshikawa, A.: FreeGaze: A gaze tracking system for everyday gaze interaction, *Proc. ACM Symposium on Eye Tracking Research & Applications (ETRA)*, pp.125–132 (2002).
- [91] Palm Pictures: Ghost In the Shell (DVD) (1998).
- [92] Pamplona, V.F., Mohan, A., Oliveira, M.M. and Raskar, R.: NE-TRA: Interactive Display for Estimating Refractive Errors and Focal Range, *ACM Trans. Graph.*, Vol.29, No.4, pp.77:1–77:8 (2010).
- [93] Pamplona, V.F., Passos, E.B., Zizka, J., Oliveira, M.M., Lawson, E., Clua, E. and Raskar, R.: CATRA: Interactive Measuring and Modeling of Cataracts, *ACM Trans. Graph.*, Vol.30, No.4, pp.47:1–47:8 (2011).
- [94] Paramount Pictures: CSI NY Season 1, Ep. 10: “Night, mother” (DVD) (2005).
- [95] Reale, M., Hung, T. and Yin, L.: Viewing direction estimation based on 3D eyeball construction for HRI, *Proc. IEEE Conference on Computer Vision and Pattern Recognition Workshops (CVPRW)*, pp.24–31 (2010).
- [96] Remington, L.A.: *Clinical Anatomy of the Visual System*, Butterworth-Heinemann, 2nd edition (2004).
- [97] Ryan, W.J., Woodard, D.L., Duchowski, A.T. and Birchfield, S.T.: Adapting starburst for elliptical iris segmentation, *Proc. IEEE International Conference on Biometrics: Theory, Applications and Systems (BTAS)*, pp.1–7 (2008).
- [98] Safaee-Rad, R., Tchoukanov, I., Smith, K.C. and Benhabib, B.: Three-dimensional location estimation of circular features for machine vision, *IEEE Trans. Robot. Autom.*, Vol.8, No.5, pp.624–640 (1992).
- [99] Salvi, J., Fernandez, S., Pribanic, T. and Llado, X.: A state of the art in structured light patterns for surface profilometry, *Pattern Recogn.*, Vol.43, No.8, pp.2666–2680 (2010).
- [100] Schindler, G.: Photometric Stereo via Computer Screen Lighting for Real-time Surface Reconstruction, *Proc. International Symposium on 3D Data Processing, Visualization and Transmission (3DPVT)* (2008).
- [101] Schnieders, D., Fu, X. and Wong, K.-Y.K.: Reconstruction of Display and Eyes from a Single Image, *Proc. IEEE Conference on Computer Vision and Pattern Recognition (CVPR)*, pp.1442–1449 (2010).
- [102] Schnieders, D., Wong, K.-Y.K. and Dai, Z.: Polygonal Light Source Estimation, *Proc. Asian Conference on Computer Vision (ACCV)*, pp.96–107 (2009).
- [103] Semple, J.G. and Kneebone, G.T.: *Algebraic Projective Geometry*, Oxford University Press (1952).
- [104] SensoMotoric Instruments GmbH (SMI): IVIEW X™HED, available from (<http://www.smivision.com/en/gaze-and-eye-tracking-systems/products/iview-x-hed.html>) (accessed 2013-01-15).
- [105] SensoMotoric Instruments GmbH (SMI): RED/RED250/RED500, available from (<http://www.smivision.com/en/gaze-and-eye-tracking-systems/products/red-red250-red-500.html>) (accessed 2013-01-15).
- [106] Shih, S.-W., Wu, Y.-T. and Liu, J.: A Calibration-Free Gaze Tracking Technique, *Proc. IEEE International Conference on Pattern Recognition (ICPR)*, pp.4201–4204 (2000).
- [107] Smart Eye AB: Smart Eye Pro 5.7, available from (<http://www.smarteye.se/productsreal-objects/smart-eye-pro-2-8-cameras>) (accessed 2012-09-30).
- [108] Smith, J.D., Vertegaal, R. and Sohn, C.: ViewPointer: Lightweight calibration-free eye tracking for ubiquitous handsfree deixis, *Proc. ACM Symposium on User Interface Software and Technology (UIST)*, pp.53–61 (2005).
- [109] Snell, R.S. and Lemp, M.A.: *Clinical Anatomy of the Eye*, Blackwell Publishing, Malden, 2nd edition (1997).
- [110] SR Research Ltd.: EyeLink 1000, available from ([http://www.sr-research.com/EL\\_1000.html](http://www.sr-research.com/EL_1000.html)) (accessed 2013-01-15).
- [111] SR Research Ltd.: EyeLink II, available from ([http://www.sr-research.com/EL\\_II.html](http://www.sr-research.com/EL_II.html)) (accessed 2013-01-15).
- [112] Stampe, D.M.: Heuristic filtering and reliable calibration methods for video-based pupil-tracking systems, *Behav. Res. Meth. Instrum. Comput.*, Vol.25, No.2, pp.137–142 (1993).
- [113] Strelow, D., Mishler, J., Koes, D. and Singh, S.: Precise Omnidirectional Camera Calibration, *Proc. IEEE Conference on Computer Vision and Pattern Recognition (CVPR)*, pp.689–694 (2001).
- [114] Sturm, P.: Mixing catadioptric and perspective cameras, *Proc. IEEE Workshop on Omnidirectional Vision (OMNIVIS)*, pp.37–44 (2002).
- [115] Sturm, P., Ramalingam, S., Tardif, J.-P., Gasparini, S. and Barreto, J.: Camera Models and Fundamental Concepts Used in Geometric Computer Vision, *Found. Trends. Comput. Graph. Vis.*, Vol.6, pp.1–183 (2011).
- [116] Svoboda, T. and Pajdla, T.: Epipolar Geometry for Central Catadioptric Cameras, *Int. J. Comput. Vision*, Vol.49, No.1, pp.23–37 (2002).
- [117] Swaminathan, R., Grossberg, M.D. and Nayar, S.K.: Non-Single Viewpoint Catadioptric Cameras: Geometry and Analysis, *Int. J. Comput. Vision*, Vol.66, No.3, pp.211–229 (2006).
- [118] Swartz, T., Marten, L. and Wang, M.: Measuring the cornea: The latest developments in corneal topography, *Curr. Opin. Ophthalmol.*, Vol.18, No.4, pp.325–333 (2007).
- [119] Tian, J. and Ma, K.-K.: A survey on super-resolution imaging, *Signal Image Video Process.*, Vol.5, No.3, pp.329–342 (2011).
- [120] Tobii Technology AB: Tobii Glasses Eye Tracker, available from (<http://www.tobii.com/en/eye-tracking-research/global/products/hardware/tobii-glasses-eye-tracker/>) (accessed 2013-01-15).
- [121] Tobii Technology AB: Tobii X60 & X120 Eye Tracker, available from (<http://www.tobii.com/en/eye-tracking-research/global/products/hardware/tobii-x60-x120-eye-tracker/>) (accessed 2013-01-15).
- [122] Tomasi, C. and Manduchi, R.: Bilateral filtering for gray and color images, *Proc. IEEE International Conference on Computer Vision*

- (*ICCV*), pp.839–846 (1998).
- [123] Tsumura, N., Dang, M.N., Makino, T. and Miyake, Y.: Estimating the directions to light sources using images of eye for reconstructing 3D human face, *Proc. IS&T/SID Color Imaging Conference (CIC)*, pp.77–81 (2003).
  - [124] Tweed, D. and Vilis, T.: Geometric relations of eye position and velocity vectors during saccades, *Vision Res.*, Vol.30, No.1, pp.111–127 (1990).
  - [125] Vandepoortael, B.: Contributions à la vision omnidirectionnelle: Etude, Conception et Etalonnage de capteurs pour l'acquisition d'images et la modélisation 3D, Thèse de doctorat, Institut National Polytechnique de Toulouse (2006).
  - [126] Vezhnevets, V. and Degtiareva, A.: Robust and accurate eye contour extraction, *Proc. Graphicon*, pp.81–84 (2003).
  - [127] Villanueva, A. and Cabeza, R.: Models for Gaze Tracking Systems, *J. Image Video Process.*, Vol.2007, No.3, pp.1–16 (2007).
  - [128] Villanueva, A. and Cabeza, R.: A novel gaze estimation system with one calibration point, *IEEE Trans. Syst. Man Cybern. Part B Cybern.*, Vol.38, No.4, pp.1123–1138 (2008).
  - [129] Villanueva, A., Daunys, G., Hansen, D.W., Böhme, M., Cabeza, R., Meyer, A. and Barth, E.: A geometric approach to remote eye tracking, *Univers. Access Inf. Soc.*, Vol.8, No.4, pp.241–257 (2009).
  - [130] Wang, H., Lin, S., Ye, X. and Gu, W.: Separating corneal reflections for illumination estimation, *Neurocomputing*, Vol.71, No.10–11, pp.1788–1797 (2008).
  - [131] Wang, J.-G. and Sung, E.: Gaze determination via images of irises, *Image Vision Comput.*, Vol.19, No.12, pp.891–911 (2001).
  - [132] Wang, J.-G. and Sung, E.: Study on eye gaze estimation, *IEEE Trans. Syst. Man Cybern. Part B Cybern.*, Vol.32, No.3, pp.332–350 (2002).
  - [133] Wildes, R.P.: Iris recognition: An emerging biometric technology, *Proc. IEEE*, Vol.85, No.9, pp.1348–1363 (1997).
  - [134] Wu, H., Chen, Q. and Wada, T.: Visual Direction Estimation from a Monocular Image, *IEICE Trans. Inf. Syst.*, Vol.E88-D, No.10, pp.2277–2285 (2005).
  - [135] Wu, H., Kitagawa, Y., Wada, T., Kato, T. and Chen, Q.: Tracking Iris Contour with a 3D Eye-Model for Gaze Estimation, *Proc. Asian Conference on Computer Vision (ACCV)*, pp.688–697 (2007).
  - [136] Würz-Wessel, A.: Free-formed Surface Mirrors in Computer Vision Systems, PhD Thesis, Universität Tübingen (2003).
  - [137] Yagi, Y.: Omnidirectional Sensing and Its Applications, *IEICE Trans. Inf. Syst.*, Vol.E82-D, No.3, pp.568–579 (1999).
  - [138] Yamazoe, H., Utsumi, A., Yonezawa, T. and Abe, S.: Remote and Head-Motion-Free Gaze Tracking for Real Environments with Automated Head-Eye Model Calibrations, *Proc. IEEE Conference on Computer Vision and Pattern Recognition Workshops (CVPRW)*, pp.1–6 (2008).
  - [139] Yoo, D.H. and Chung, M.J.: A novel non-intrusive eye gaze estimation using cross-ratio under large head motion, *Comput. Vis. Image Underst.*, Vol.98, No.1, pp.25–51 (2005).
  - [140] Young, L. and Sheena, D.: Survey of eye movement recording methods, *Behav. Res. Meth. Instrum.*, Vol.7, No.5, pp.397–429 (1975).
  - [141] Zhang, L., Subramaniam, N., Lin, R., Raskar, R. and Nayar, S.: Capturing Images with Sparse Informational Pixels using Projected 3D Tags, *Proc. IEEE Virtual Reality Conference (VR)*, pp.11–18 (2008).
  - [142] Zheng, Y., Ma, W. and Liu, Y.: Another way of looking at monocular circle pose estimation, *Proc. IEEE International Conference on Image Processing (ICIP)*, pp.861–864 (2008).



**Atsushi Nakazawa** received a B.S. and Ph.D. in Engineering from Osaka University, Japan in 1997 and 2001 respectively. In 2001 he joined the Institute of Industrial Science, the University of Tokyo as a postdoctoral researcher. Since 2003 he is working at Cybermedia Center, Osaka University as a lecturer. From 2007 to

2008 he was a visiting researcher at Georgia Institute of Technology, US. From 2010 he is a PRESTO (Precursory Research for Embryonic Science and Technology) researcher in Japan Science and Technology Agency (JST). His research interests include computer vision, robotics and human interfaces; in particular, estimating human posture from images, analysis of human motion using motion capture, humanoid robot control, image-based eye analysis, and eye gaze tracking. He is a member of IEEE, IPSJ and RSJ.



**Haruo Takemura** received a B.S., M.S. and Ph.D. in Engineering from Osaka University, Japan in 1982, 1984 and 1987 respectively. In 1987 he joined Advanced Telecommunication Research Institute, International. In 1994 he joined Nara Institute of Science and Technology as associate professor at Graduate School

of Information Science and Technology. From 1998 to 1999 he was a visiting associate professor at University of Toronto, Canada. In 2001 he became a full professor at Cybermedia Center, Osaka University. From 2005 to 2007, and again since 2011 he also serves as vice-director and from 2007 to 2011 as director of Cybermedia Center. His research interests include interactive computer graphics, human-computer interaction and mixed reality. He is a member of IEICE, IPSJ, VRSJ, HIS, ITE, IEEE and ACM.

(Communicated by *Koichiro Deguchi*)



**Christian Nitschke** received a Diploma (M.S.) in Media Systems from the Bauhaus Universität Weimar, Germany in 2006 and a Ph.D. in Engineering from Osaka University, Japan in 2011. He is currently a postdoctoral research fellow at Cybermedia Center, Osaka University. Meanwhile, he worked for VIOSO GmbH

Germany, creating software solutions for multi-projector displays and projection onto arbitrary surfaces. His research interests include computer vision, visualization/display technologies and human interfaces. In particular, 3D reconstruction, scene understanding, image-based eye analysis and eye gaze tracking.